INTERNAL TIDES OFF SOUTHERN CALIFORNIA

Analysis of data obtained by NEL thermistor chain

W. Krauss • Research and Development Report • 6 July 66

U. S. NAVY ELECTRONICS LABORATORY, SAN DIEGO, CALIFORNIA

NEL/REPORT 1389

PROBLEM

Investigate and report on the nature of internal waves in the sea. Specifically, study the differences between spectra of internal waves as obtained from an anchor station and those measured by a towed thermistor chain, and apply the results to internal tides in the sea off southern California.

RESULTS

1. A method accounting for doppler-shift effects was used to interpret data recorded from San Diego to Hawaii by moving thermistors. The results lead to a reasonable picture of the internal tides in that area of the Pacific Ocean.
2. It is shown that internal waves can be produced directly by the tide-generating forces. Free diurnal internal waves vanish at 30°N.
3. Internal tidal waves are an important component in the spectra at tidal frequencies in the sea off southern California. It is likely that they travel in a northeasterly direction.

RECOMMENDATIONS

1. Verify the theory of internal waves of tidal period with additional measurements with the thermistor chain.
2. For a complete analysis of the various modes of internal waves, extend measurement of the thermal structure to the sea floor.
3. Supplement the study of internal waves by the use of current meters and salinometers mounted on the chain or at anchored stations; use the data produced to increase the usefulness of thermistor-chain data in the study of the ocean structure (sound-velocity structure) controlled by non-periodic motion such as advection.

ADMINISTRATIVE INFORMATION

Work was performed under SR 104 03 01, Task 0580 (NEL L40461). The report covers work from August 1963 to February 1964 and was approved for publication 6 July 1966.

Financial arrangements for travel and salary were furnished by ONR and administered by Scripps Institution of Oceanography.

The author is grateful for the assistance of E. Good, J. R. Olson, D. L. Jackson, C. L. Barker, and P. G. Hansen in collecting data; of Mrs. R. P. Brown and R. F. Arenz in programming and computer analysis; of R. McKinley, J. Larson, and Mrs. A. Moore in computations and plotting; and of O. S. Lee, G. H. Curl, and E. C. LaFond, who reviewed the manuscript.

CONTENTS

TABLES

ILLUSTRATIONS

ILLUSTRATIONS (continued)

LIST OF SYMBOLS

A_n	$(a_n^2 + b_n^2)^{1/2}$ = rms amplitude of the Fourier components
a_n, b_n	Fourier amplitudes
A_n, B_n	Amplitudes of the modes, $W_n(z)$, of an internal wave
c	ω/κ, phase velocity
f	Coriolis parameter = $2\Omega \sin \Phi$ where Ω is the angular frequency of the earth and Φ is the latitude
g	Acceleration of gravity
H	Bottom depth
h	Horizontal component, used as an index
k_0	Amplitude of the inhomogeneous term responsible for the development of internal tides (magnitude 10^{-28} cm^{-1} sec^{-3})
$k_{\ell,m}$	Fourier components of k_0
K_0	Amplitude of the tide-generation force
ℓ, m	Integers in Fourier expansions
P	$p/\bar{\rho}$
p	Pressure
S	Salinity
T	Temperature
U	Ship's velocity
$\vec{v}$	(u,v,w) = velocity vector
$w(x,y,z,t)$	$\overset{\circ}{w}(x,y,z) \exp(i\omega t) = w(z)G(x,y) \exp(i\omega t) = w(z)G(x)G(y) \exp(i\omega t)$ vertical velocity
$W_n(z)$	Modes of the eigenfunctions, describing the vertical dependency of an internal wave with the vertical velocity $w(x,y,z,t)$

x,y,z	Right-handed rectangular coordinate system, z pointing downward
a	Angle between the ship's direction and the direction of wave travel
$\Gamma(z)$	$\frac{1}{\bar{\rho}} \frac{d\bar{\rho}}{dz}$
δ	Delta function
ϵ	Eigenvalue
ζ	w/ω = amplitude of the displacement
Θ	Potential temperature
κ,η	Wave number in x, y direction
λ	Wavelength
μ	Weighting factor in the eigenfunction expansion for unequally spaced data
ξ	A transformation (see equation 76)
ρ	Density
$\bar{\rho}(z)$	Mean density distribution
σ_t	$\bar{\rho}\ [(S,T,p=0)] \cdot 10^3$
τ	Period
τ'	Doppler-shifted period
Υ	A transformation (see equation 79)
ϕ	Phase of a wave, gravitational potential or geographical latitude
ψ	A wave function of (x,y,z,t)
$\overset{\circ}{\psi}$	Space-dependent part of the wave function
ω	$\frac{2\pi}{\tau}$ = angular frequency

INTRODUCTION

It was shown by A. Defant[1] in 1950 that internal tides strongly influence the hydrographic situation in the area off California. Since then, various measurements were made of internal waves in this area,[2-4] but the studies did not produce details of the modes of these internal tides, nor of their origin and direction of progress in the open sea. Studies of near-coast areas[5,6] showed that no constant phase lag exists between surface tides and internal tides. In 1963, Summers and Emery[7] conducted a multiple-ship study in the area off southern California, and on the basis of their measurements formulated a very reasonable picture of the semidiurnal tidal waves in that area. However, their values for phase velocity are not in complete agreement with the values derived from the theory of internal waves. For instance, their recorded component of the phase velocity is about 9 knots in deep water and 0.6 knot over the shallow shelf – values corresponding to about 4.6 meters/sec and 0.31 meter/sec. A reasonable value for the first mode, according to hydrodynamic theory, would be 1.6 meters/sec for the semidiurnal wave. The reason for this discrepancy seems to be that Summers and Emery disregarded the diurnal internal tides, which play an important role in their records, as can be seen immediately in those from the R.V. Velero IV and USS EXCEL.

The study to be reported here was undertaken to gain a broader understanding of internal tides – their natural movements, and the effects of doppler shift upon the direction of their propagation. The areas studied included various points off southern California and a long section from San Diego to the Hawaiian Islands.

The data were obtained by use of the NEL thermistor chain,[8] a towed instrument which records nearly continuous temperature data from the surface to a depth of about 230 meters. The measurements are recorded in analog form as depths of isotherms. Depending on the information sought, the towing ship followed an X-pattern, drifted, or lay at anchor.

The following sections will present: (1) development of equations necessary for the analysis of the doppler shift of internal waves, (2) development of an equation expressing the nature of free and forced internal tides in the open sea, (3) analysis of the chain data collected from towed, anchor, and drifting stations off southern California, and (4) analysis of the chain data in a long section from San Diego to the Hawaiian Islands.

---

[1]Superscript numbers identify references listed at end of report.

ANALYSIS OF FIXED AND TOWED OBSERVATIONS OF INTERNAL WAVES

Importance of the Phase Velocity

Any small perturbation in an inviscid, incompressible area of the ocean, where currents can be neglected, is determined by the equation

$$\nabla_h^2 \frac{\partial^2 w}{\partial t^2} + g\Gamma \nabla_h^2 w + \frac{\partial^4 w}{\partial z^2 \partial t^2} + f^2 \frac{\partial^2 w}{\partial z^2} + \Gamma \left(\frac{\partial^3 w}{\partial z \partial t^2} + f^2 \frac{\partial w}{\partial z} \right) = 0 \quad (1)$$

with the boundary conditions

$$w = 0 \text{ at } z = 0 \quad (2)$$

and

$$w = u \frac{\partial H}{\partial x} + v \frac{\partial H}{\partial y} \text{ where } z = H(x,y) \quad (3)$$

Equation 1 follows from hydrodynamic equations, the continuity equation, and the incompressibility condition. Surface waves are excluded.

In the following sections we restrict ourselves to water areas of constant depth: $H(x,y) = H$ = constant. Expanding w into a Fourier series,

$$w(x,y,z,t) = \sum_{k,\ell,m} W_{k,\ell,m}(z) \exp \left[i \left(\kappa_k x + \eta_\ell y + \omega_m t \right) \right] \quad (4)$$

we get for the vertical dependency $W_{k,\ell,m}(z)$

$$\begin{cases} \dfrac{d^2W}{dz^2} + \Gamma \dfrac{dW}{dz} + \dfrac{g\Gamma - \omega^2}{\omega^2 - f^2} (\kappa^2 + \eta^2) W = 0 \\ W = 0 \text{ at } z = 0 \text{ and } z = H \end{cases} \quad (5)$$

where the indices have been dropped.

Long waves are characterized by $g\Gamma >> \omega^2$. Furthermore, long waves can be assumed to be long-crested. If they travel in the x direction, we then have $\kappa^2 >> \eta^2$ and equation 5 reduces to

$$\begin{aligned} &\frac{d^2W}{dz^2} + \Gamma \frac{dW}{dz} + \Gamma \epsilon W = 0 \\ &W = 0 \text{ at } z = 0 \text{ and } z = H \end{aligned} \quad (6)$$

with the eigenvalues

$$\epsilon_n = \frac{g\kappa_n^{\,2}}{\omega^2 - f^2} \tag{7}$$

The vertical dependency of the observed fluctuations in the ocean are then described by

$$W(z) = \sum_{n=1}^{\infty} A_n W_n(z) \tag{8}$$

The phase velocity of these waves, c_n is given by

$$c_n = \frac{\omega}{\kappa_n} = \left[\frac{g}{\epsilon_n \left(1 - \frac{f^2}{\omega^2} \right)} \right]^{1/2} \tag{9}$$

if $f^2 << \omega^2$, equation 9 reduces to

$$c_n = \left(\frac{g}{\epsilon_n} \right)^{1/2} \tag{10}$$

Therefore, the phase velocity can be computed simply by measuring the mean density $\bar{\rho}(z)$ and computing the eigenvalues ϵ_n from (6). $\Gamma(z)$ is generally computed from the formula

$$\Gamma(z) \approx \frac{1}{1+10^{-3}\sigma_t} \frac{1}{\Delta z} \sigma_t(z + \Delta z) - \sigma_t(z) \tag{11}$$

Analysis of Data from Anchor Stations

Knowledge of the internal wave structure of an area is best obtained at anchor stations, where doppler shifting will not affect the frequencies and where observations can extend to the bottom. The thermistor chain is ideally suited for observations from an anchored ship in shallow water because its temperature sensors are equally spaced. Equal spacing of transducers is essential because description of observations by internal waves requires

$$\int_0^H \left[a(z) - \sum_{n=1}^{N} A_n W_n(z) \right] W_r(z) dz = 0, \text{ for } r = 1,2,\ldots N \qquad (12)$$

from which, for numerical calculations,

$$\sum_{\Delta z_i} \left[a(z) - \sum_{n=1}^{N} A_n W_n(z_i) \right] W_r(z_i)\, \Delta z_i = 0, \text{ for } r = 1,2,\ldots N \qquad (13)$$

follows. This equation reduced to (19) only in the case where Δz_i = constant. If this is not valid, the weighting factors, Δz_i, influence the result considerably. Let q be the number of depths for which the amplitudes, $a(z_i)$, have been determined. For depth range

$$\Delta z_i = \frac{(z_{i+1} - z_{i-1})}{2} ,$$

$a(z_i)$ is supposed to be representative. The whole column is divided into $(q+1)$ subranges and instead of using Δz_i in equation 13 we can use, after multiplication by $q+1/H$ the dimensionless weighting factors

$$\mu_i = \frac{\Delta z_i}{H/(q+1)} = \frac{(z_{i+1} - z_{i-1})(q+1)}{2H} \qquad (14)$$

The weighting factors are 1 for equally spaced Δz_i, that is for

$$H = \frac{(q+1)(z_{i+1} - z_{i-1})}{2}$$

Many computations have shown that disregarding the weighting factors (14) leads to erroneous results and further study is recommended.

Following is a summary of the formulas needed for processing data taken from records at an anchor station. These will permit comparison of spectra from an anchor station and those from towed instruments.

Suppose we have observed the temperature fluctuation, $T(t_i, z_i)$, at an anchor station at the levels z_i. From the mean temperature distribution, $\overline{T}(z)$, it follows that the displacement of the particles from their mean position is given by

$$\zeta(t_i, z_i) = \frac{T(t_i, z_i)}{(d\overline{T}/dz)_i} \qquad (15)$$

From Fourier analysis we find the amplitudes, a and b, for a distinct frequency, ω:

$$\zeta(t, z_i) = a(z_i) \cos \omega t + b(z_i) \sin \omega t \qquad (16)$$

In order to interpret these fluctuations as internal waves we assume $W = \omega\zeta$; then

$$a(z_i) = \sum_{n=1}^{N} A_n^* \zeta_n(z_i) = \sum_{n=1}^{N} A_n W_n(z_i) \tag{17}$$

where

$$A_n = \frac{A_n^*}{\omega},\ A_n^* \zeta_n = A_n W_n$$

To find the amplitude A_n, we use the method of least squares. If the depths, z_i, are equally spaced,

$$\sum_{i=1}^{I} \left[a(z_i) - \sum_{n=1}^{N} A_n W_n(z_i) \right]^2 = \text{Minimum} \tag{18}$$

must hold; this yields the system of equations

$$\sum_{i=1}^{I} \left[a(z_i) - \sum_{n=1}^{N} A_n W_n(z_i) \right] W_r(z_i) = 0, \text{ for } r = 1,2,\ldots N \tag{19}$$

from which the A_n are determined by using a computer. Equations for $b(z_i)$ and B_n have a form similar to equations 17 and 19 and are therefore not shown here. Equations 6 and 10 are used to find the phase velocities and equation 19 is used to compute amplitude of the modes. The study of modes of internal waves from anchor stations in shallow water is greatly facilitated when the observations extend to the bottom. This basic insight into the internal wave structure of an area is generally obtained by anchor stations because the records contain no doppler-shifted frequencies.

Doppler Shifts of a Single Internal Wave Using a Moving Sensor

We assume that there is only one internal wave present with the period τ. If the ship is anchored at $x = x_0$, it can easily measure this period τ.

Case 1: Suppose the ship travels with the speed U in the $+x$ direction, and the wave moves with the velocity c_x in the direction $-x$. Then we have a doppler shift and observe the apparent period τ', given by

$$\tau' = \frac{\tau}{1 + \frac{U}{c_x}} \tag{20}$$

where U = ship's velocity. With increasing ship velocity, U, the apparent period gets shorter.

$$0 \leqq \tau' \leqq \tau \quad \text{for } U \gtrless c_x \text{ and } c_x > 0 \tag{21}$$

Case 2: If the wave travels in the same direction, $+x$, as the ship, then we have

$$\tau' = \frac{\tau}{1 - \frac{U}{c_x}} \tag{22}$$

with

$$\tau \leqq \tau' \leqq \infty \text{ for } U \leqq c_x \text{ and } c_x > 0 \tag{23}$$

With $U > c_x$, we again have Case 1 because the phase velocity of the wave is negative relative to the ship's velocity.

Generally, in Case 2, we find

$$0 \leqq \tau' \leqq \infty \text{ for } U \gtrless c_x \text{ and } c_x > 0 \tag{24}$$

Case 3: If the wave travels with the velocity, c, in any direction which makes an angle, α, with the ship's direction, then the effective ship's velocity is

$$U_{\text{eff.}} = U \cos \alpha \tag{25}$$

and we generally write, for the period τ':

$$\tau' = \frac{\tau}{\left|1 - \frac{U \cos \alpha}{c}\right|} \tag{26}$$

with

$$0 < \tau' \leqq \infty \text{ for } 0 \leqq \alpha \leqq 2\pi$$

It is seen from equation 26 that with $\alpha = 90^{\circ}$ we get $\tau' = \tau$ as in the case of an anchor station.

Equation 26 shows that with no prior knowledge of the direction of progress of the wave there is no possibility to filter the record because the period τ may appear at any value τ'. In (26) the unknowns are τ and α. The velocity, U, of the ship is known and phase velocity of an internal wave at any period is given by its eigenvalue. τ' is recorded. In order to determine τ and α we have to carry out the cruise pattern as shown in figure 1.

We define the angle α_0,

$$\frac{U}{c} \cos \alpha_0 = 1 \text{ for } 0 \leqq \alpha_0 \leqq \frac{\pi}{2}$$

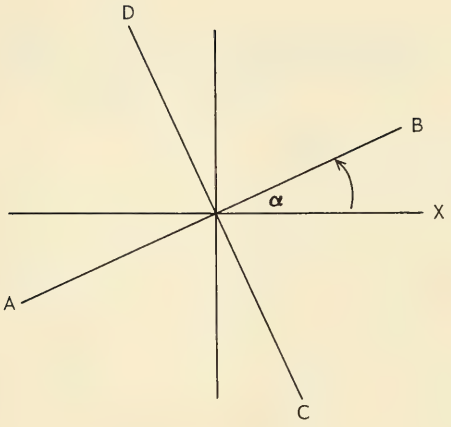

Figure 1. Cruise pattern AB, BA, CD, DC.

U and c are known; therefore, α_0 is also known. Consider cases (a), (b), and (c), as follows:

(a) If $\frac{U}{c}\cos\alpha \leqq +1$, then

$$\tau' = \frac{\tau}{1 - \frac{U}{c}\cos\alpha}$$

holds. From the legs AB, BA, CD, and DC in figure 1 we have

$$\tau'_{AB} = \frac{\tau}{1 - \frac{U}{c}\cos\alpha} \qquad \tau'_{BA} = \frac{\tau}{1 + \frac{U}{c}\cos\alpha}$$

$$\tau'_{DC} = \frac{\tau}{1 - \frac{U}{c}\sin\alpha} \qquad \tau'_{CD} = \frac{\tau}{1 + \frac{U}{c}\sin\alpha}$$

From these formulas we get

$$\tau = \frac{2\tau'_{AB}\,\tau'_{BA}}{\tau'_{AB} + \tau'_{BA}} = \frac{2\tau'_{CD}\,\tau'_{DC}}{\tau'_{CD} + \tau'_{DC}} \tag{27}$$

and

$$\sin \alpha = \frac{c}{U}\left(\frac{\tau'_{DC} - \tau'_{CD}}{\tau'_{CD} + \tau'_{DC}}\right), \quad \cos \alpha = \frac{c}{U}\left(\frac{\tau'_{AB} - \tau'_{BA}}{\tau'_{AB} + \tau'_{BA}}\right) \tag{28}$$

The ranges for α are shown in figure 2.

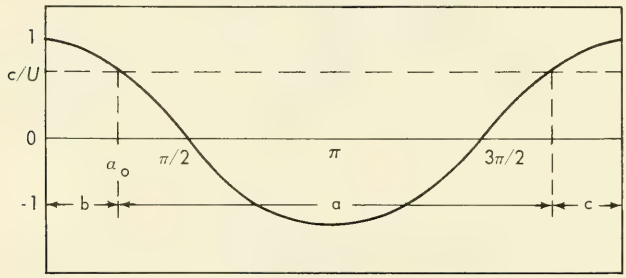

Figure 2. Graphical presentation of the cases (a), (b), and (c).

If $\frac{U}{c}\cos \alpha > 1$ holds, we have to distinguish two possibilities depending on α:

(b) If $\frac{U}{c}\cos \alpha > 1$ and $0 \leqq \alpha \leqq \frac{\pi}{2}$,

we have

$$\tau' = \frac{\tau}{\frac{U}{c}\cos \alpha - 1}$$

and with

$$\alpha_0 \gtrless \pi/4$$

the result is

$$\tau'_{AB} = \frac{\tau}{\frac{U}{c}\cos \alpha - 1}, \qquad \tau'_{DC} = \frac{\tau}{\pm\frac{U}{c}\sin \alpha \mp 1}$$

where the upper sign holds for $\alpha_0 > \pi/4$ and $\alpha > \pi/2 - \alpha_0$; the lower one holds for $\alpha_0 > \pi/4$ and $\alpha < \pi/2 - \alpha_0$ or $\alpha_0 < \pi/4$ and α arbitrary. From these formulas follows

$$\tau = -\tau'_{AB}\,\tau'_{DC}\,\frac{\tau'_{DC} \pm \tau'_{AB}}{\tau'^2_{AB} + \tau'^2_{DC}} + \left[\tau'_{AB}\,\tau_{DC}\left(\frac{\tau'_{DC} \pm \tau'_{AB}}{\tau'^2_{AB} + \tau'^2_{DC}}\right)^2 + \frac{\tau'^2_{AB}\,\tau'^2_{DC}}{\tau'^2_{AB} + \tau'^2_{DC}}\left(\frac{U^2}{c^2} - 2\right)\right]^{1/2} \tag{29}$$

$$\sin\alpha = \frac{c}{U}\left(1 \pm \frac{\tau}{\tau'_{DC}}\right),\ \cos\alpha = \frac{c}{U}\left(1 + \frac{\tau}{\tau'_{AB}}\right) \tag{30}$$

(c) If $\frac{U}{c}\cos\alpha > 1$ and $\frac{3}{2}\pi \leq \alpha \leq 2\pi$, the equations

$$\tau'_{AB} = \frac{\tau}{\frac{U}{c}\cos\alpha - 1}\ ,\qquad \tau'_{CD} = \frac{\tau}{\mp\frac{U}{c}\sin\alpha \mp 1}$$

must hold, where the upper sign is valid for $\alpha_0 < \frac{\pi}{4}$ and $\alpha < \frac{3}{2}\pi + \alpha_0$, the lower sign valid for $\alpha_0 > \pi/4$ and $\alpha > \frac{3}{2}\pi + \alpha_0$ or $\alpha_0 > \pi/4$ and α arbitrary. The period again is given by equation 29, substituting τ'_{DC} by τ'_{CD} , the angle is determined by

$$\sin\alpha = -\frac{c}{U}\left(1 \pm \frac{\tau}{\tau'_{CD}}\right),\ \cos\alpha = \frac{c}{U}\left(1 + \frac{\tau}{\tau'_{AB}}\right) \tag{31}$$

Doppler Shifts for an Infinite Number of Modes of an Internal Wave with a Period τ

So far one internal wave with the period τ and phase velocity c has been considered. A case will now be considered where there is again only one period τ_0 but the wave is composed of different modes as is the case for all real internal waves.

Case 1: If the process is observed at the anchor station, we record the fluctuations

$$F(z, t) = \sum_{n=1}^{N}\left[A_n W_n(z)\cos\frac{2\pi}{\tau_0}t + B_n W_n(z)\sin\frac{2\pi}{\tau_0}t\right] \tag{32}$$

where

$$a(z) = \sum_{n=1}^{N} A_n W_n(z) \ , \ b(z) = \sum_{n=1}^{N} B_n W_n(z)$$

are the observed amplitudes of the cosine and sine components. The amplitude and phase spectra are given by

$$A(\omega, z) = \begin{cases} \left(\left[\sum_n A_n W_n(z) \right]^2 + \left[\sum_n B_n W_n(z) \right]^2 \right)^{1/2} & \text{for } \omega = \omega_0 \\ 0 \text{ elsewhere} \end{cases} \tag{33}$$

$$\phi(\omega, z) = \begin{cases} \arctan \dfrac{\sum B_n W_n(z)}{\sum_n A_n W_n(z)} & \text{for } \omega = \omega_0 \\ \text{not defined elsewhere} \end{cases}$$

where $A(\omega,z)$ is the amplitude density and should not be confused with A_n. A schematic of the amplitude $A(\omega,z)$ is given in figure 3.

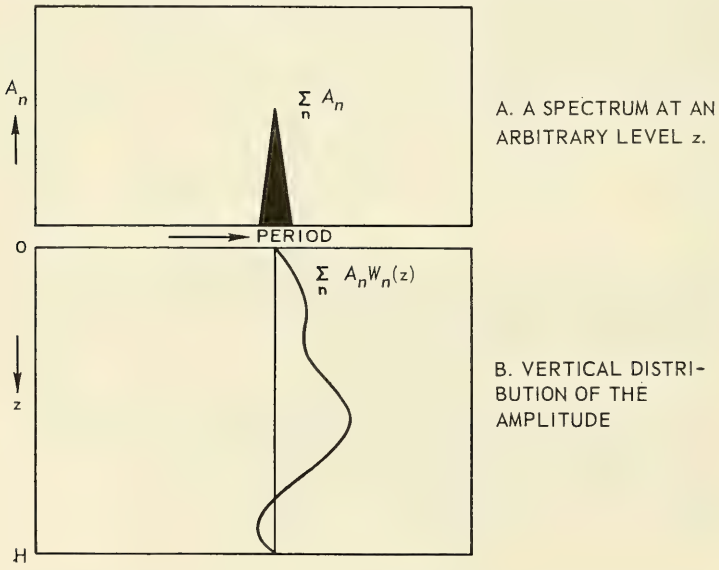

Figure 3. Schematic diagram of an observed amplitude distribution $A_n W_n(z)$ at an anchor station (eqn. 32).

Amplitude and phase spectra are quite different in Case 2 where an internal wave of many modes but of a single frequency, ω_0, is observed by using transducers that are in motion.

Case 2: Because of the different phase velocity c_n of each mode we get the periods

$$\tau'_{0,n} = \frac{\tau_0}{\left|1 - \frac{U \cos \alpha}{c_n}\right|} \tag{34}$$

if α is the same for all c_n. The process is recorded as

$$F'(z, t) = \sum_{n=1}^{N} \left[A_n W_n(z) \cos \frac{2\pi}{\tau'_{0,n}} t + B_n W_n(z) \sin \frac{2\pi}{\tau'_{0,n}} t \right] \tag{35}$$

This record is much more complicated because a complete set of apparent periods, $\tau'_{0,n}$ for $n = 1, 2, 3, \ldots N$, is recorded instead of one period that would be recorded at a fixed point. Amplitude and phase spectra are given by

$$A(\omega', z) = \begin{cases} \left(A_n^2 + B_n^2\right)^{1/2} W_n(z) \text{ for } \omega' = \omega'_{0,n} = \dfrac{2\pi}{\tau'_{0,n}} \\ \\ 0 \text{ elsewhere} \end{cases}$$

$$\phi(\omega', z) = \begin{cases} \arctan \dfrac{B_n}{A_n} & \text{for } \omega' = \omega'_{0,n} \\ \\ \text{not defined elsewhere} \end{cases} \tag{36}$$

with $n = 1, 2, \ldots N$.

Figure 4 shows the same schematic amplitude spectrum as in figure 3 with $N = 4$, using a towed sensor. Because of towing, the internal wave of the period τ_0 is decomposed into the different modes which now occur at different apparent frequencies $\omega'_{0,n}$. It may be mentioned that the integral over the entire ω range of equation 33 is different from the integral of the entire ω' range in equation 36.

Case 3: Several internal waves are considered with periods τ_m which travel in the directions α_m, each one composed of a sum of different orders n. Since the ship is moving, the apparent periods $\tau_{m,n}$ are given by

$$\tau'_{m,n} = \frac{\tau_m}{\left|1 - \frac{U}{c_n} \cos \alpha_m\right|} \tag{37}$$

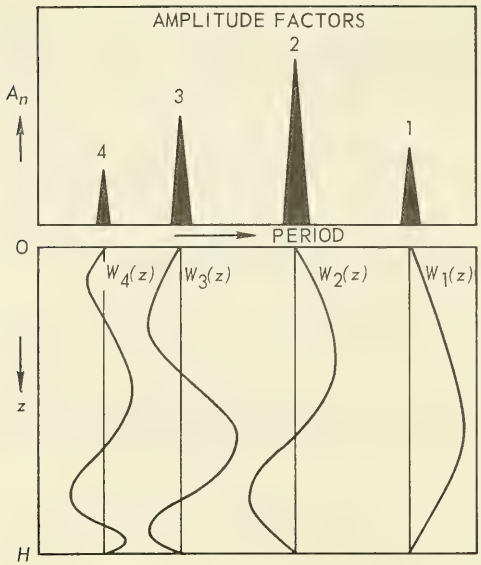

Figure 4. Schematic diagram of an observed amplitude distribution $(A_n^2 + B_n^2)^{1/2}$ *from observations made with moving thermistors.*

The process is recorded as

$$F'(z, t) = \sum_{m=0}^{M} \sum_{n=1}^{N} \left[A_{n,m} W_n(z) \cos \frac{2\pi}{\tau'_{n,m}} t + B_{n,m} W_n(z) \sin \frac{2\pi}{\tau'_{n,m}} t \right] \quad (38)$$

and as long as all $\tau'_{n,m}$ are different,

$$A(\omega', z) = \begin{cases} \left[A_{n,m}^2 + B_{n,m}^2 \right]^{1/2} W_n(z) \text{ for } \omega' = \omega'_{n,m} = \dfrac{2\pi}{\tau'_{n,m}} \\ 0 \text{ elsewhere} \end{cases} \quad (39)$$

$$\phi(\omega', z) = \begin{cases} \arctan \dfrac{B_{n,m}}{A_{n,m}} \text{ for } \omega' = \omega'_{n,m} \\ \text{not defined elsewhere} \end{cases} \quad (40)$$

Now each period τ_m produces a whole set of spikes similar to those shown in figure 4. In general, several apparent periods may coincide. For two internal waves with different periods τ_m and $\tau_{m^*}^*$, each one composed of eigenfunctions of the order n and n^*, apparent periods are coincident, *i.e.*,

$$\tau_{n,\,m} = \tau_{n^*,\,m^*}^*, \quad \text{if}$$

$$\frac{\tau_m}{\tau_{m^*}^*} = \frac{\left| 1 - \frac{U}{c_n} \cos \alpha_m \right|}{\left| 1 - \frac{U}{c_{n^*}^*} \cos \alpha_{m^*}^* \right|} \tag{41}$$

is fulfilled. In this case we find instead of (38) and (39),

$$A(\omega', z) = \begin{cases} \left(\left[\sum_{n,m} A_{n,\,m} W_n(z) \right]^2 + \left[\sum_{n,m} B_{n,\,m} W_n(z) \right]^2 \right)^{1/2} & \text{for } \omega' = \omega'_{n,\,m} = \dfrac{2\pi}{\tau'_{n,\,m}} \\ 0 \text{ elsewhere} \end{cases}$$

$$\phi(\omega', z) = \begin{cases} \arctan \dfrac{\sum_{n,m} B_{n,\,m} W_n(z)}{\sum_{n,m} A_{n,\,m} W_n(z)} & \text{for } \omega' = \omega'_{n,\,m} \\ \text{not defined elsewhere} \end{cases} \tag{42}$$

Again the apparent spectrum $A(\omega', z)$ reflects separation into the different modes similar to the case given by equation 33. Amplitudes of the modes are not given directly. The method of least squares is used for computation of $A_{n,\,m}$ and $B_{n,\,m}$.

All these considerations have dealt only with one section, for example section AB, of figure 1. The main problem is to find the apparent periods $\tau'^{(1)}_{m,n}$, $\tau'^{(2)}_{m,n}$ in the spectra for the different legs which belong together. Whether this is possible or not depends on the form of the true spectrum. A peak in the true spectrum will occur as an identical peak but at a different apparent period in each of the spectra from two different legs. These peaks must be identified in order to use equations 27, 28, and 30 for τ and α. Until now, records have been available only from rather complicated areas. In this case we have not been able to identify peaks of different legs.

The same could be shown for the power spectrum, $P(\omega,z)$, instead of the amplitude spectra. Consider a real situation, given by

$$\begin{aligned} F(z, t) &= \sum_{n=1}^{N} \left[A_n W_n(z) \cos \omega_0 t + B_n W_n(z) \sin \omega_0 t \right] \\ &= \sum_{n=1}^{N} \left[C_n W_n(z) \cos (\omega_0 t - \alpha_n(z)) \right] \end{aligned} \tag{43}$$

The chain, even in this simple case, gives a complicated pattern:

$$F'(z,t) = \sum_{n=1}^{N} \left[A_n W_n(z) \cos \omega'_n t + B_n W_n(z) \sin \omega'_n t \right]$$

$$= \sum_{n=1}^{N} \left[C_n W_n(z) \cos(\omega' t - \alpha_n(z)) \right] \tag{44}$$

with

$$\omega_0 = \frac{2\pi}{\tau_0}, \quad \omega'_{n,0} = \frac{2\pi}{\tau'_{n,0}}, \quad \tau'_{n,0} = \frac{\tau_0}{\left| 1 - \frac{U}{c_n} \cos \alpha \right|} \tag{45}$$

The power spectra for infinitely long series of the type given in equations 43 and 44 are, respectively

$$P(\omega,z) \cong 1/4 \left(\sum_{n=1}^{N} C_n W_n(z) \right)^2 \left[\delta(\omega-\omega_0) + \delta(\omega+\omega_0) \right] \tag{46}$$

$$P(\omega',z) \cong 1/4 \sum_{n=1}^{N} \left(C_n W_n(z) \right)^2 \left[\delta(\omega-\omega_n) + \delta(\omega+\omega_n) \right] \tag{47}$$

In reality (see equation 46), the energy of the internal waves is equal to the square of the sum of the mode amplitudes. The power spectrum of a thermistor chain record leads, however, to the sum of the square of the amplitudes of each mode. The total energy obtained by integration over the whole range is, according to equation 46, given by

$$P_{\text{total}}(z) = 1/2 \left[\sum_{n=1} C_n W_n(z) \right]^2 \tag{48}$$

Equation 47 yields, however,

$$P'_{\text{total}}(z) = 1/2 \sum_{n=1}^{N} C_n^2 W_n^2(z) \tag{49}$$

and therefore

$$P'_{\text{total}}(z) \neq P_{\text{total}}(z) \tag{50}$$

That is, the total energy or variance recorded with the thermistor chain is different from the actual variance or energy in the ocean.

Example:

If

$$W_n(z) = \sin \frac{n\pi z}{H}, \quad C_n = (-1)^n/n$$

then at $z = H/2$ we get

$$P_{\text{total}} = 1/2 \lim_{n\to\infty} \left[\sum_n (-1)^n \, 1/n \sin n\pi/2 \right]^2 = 1/2 \;\; \pi/16 \text{ and}$$

$$P'_{\text{total}} = 1/2 \lim_{n\to\infty} \sum_n 1/n^2 \sin^2 (n\pi/2) = 1/2 \;\; \pi^2/8$$

In this case, the energy with the chain is twice the actual energy. Choosing

$$C_n = \begin{cases} (-1)^n \text{ for } n \leq 5 \\ 0 \text{ for } n > 5 \end{cases}$$

we get

$$P_{\text{total}} = 1/2$$

$$P'_{\text{total}} = 3/2$$

NATURE OF FORCED AND FREE INTERNAL TIDES IN THE OCEAN

It has been shown by A. Defant[1,9] and B. Haurwitz[10] that, for a two-layered ocean, forced internal tidal waves in an unlimited ocean play no role outside of a very narrow band at those geographical latitudes where $\omega_0 = f$. The definitions of these symbols are: ω_0 = frequency of the tide-generating force and $f = 2\Omega \sin\phi$. At these latitudes, however, the wavelength goes to infinity. Therefore, it is believed that internal tidal waves are not forced waves. Taking the tide-generating force as

$$K_0 \exp\left[i\,(\kappa x + \omega_0 t)\right] \tag{51}$$

the Defant-Haurwitz theory shows the following unrealistic property: the tide-generating forces on the earth have a wavelength $\lambda_0 = 2\pi/\kappa_0$, which is generally larger than the ocean basins. The ocean itself, however, is assumed to be infinite. Therefore, the wavelength λ_0 should also be infinite and this means that equation 51 should be reduced to $K_0 \exp(i\,\omega_0 t)$.

A more realistic model can be obtained in the following way. Assume (1) that the wavelength λ_0 is larger than any ocean on the earth and not a multiple of the length of the ocean: $\lambda_0 > 2L$ and $\lambda_0 \neq 2nL$; and (2) that the tide-generating force can be expanded into its Fourier components in regard to the basin.

Forced Internal Waves

Starting with the perturbation equations,

$$\bar{\rho}\frac{\partial \vec{v}}{\partial t} + \vec{f} \times \vec{v}\bar{\rho} + \nabla p + \rho \nabla \phi + \vec{K} = 0 \tag{52}$$

$$\frac{\partial \rho}{\partial t} + w\frac{\partial \bar{\rho}}{\partial z} = 0$$

$$\nabla \cdot \vec{v} = 0$$

and eliminating the horizontal components of velocity, pressure, p, and density, ρ, in order to get a differential equation for the vertical component of velocity w:

$$\nabla_h^2 \frac{\partial^2 w}{\partial t^2} + g\Gamma \nabla_h^2 w + \frac{\partial^4 w}{\partial z^2 \partial t^2} + f^2 \frac{\partial^2 w}{\partial z^2} + \Gamma\left(\frac{\partial^3 w}{\partial z\, \partial t^2} + f^2 \frac{\partial w}{\partial z}\right)$$

$$= -1/\bar{\rho}\left[\nabla_h^2 \frac{\partial K_z}{\partial t} - f\left(\nabla \times \frac{\partial \vec{K}}{\partial z}\right)_z - \nabla_h \cdot \frac{\partial^2 \vec{K}}{\partial z\, \partial t}\right] \tag{53}$$

Surface tides are excluded from the boundary conditions so that in the case of a horizontal bottom

$$w = 0 \quad \text{for } z = 0 \quad \text{and} \quad z = H \tag{54}$$

must hold.

The inhomogeneous term in (53) is simplified to

$$k_0 \exp\left[i(\kappa_0 x + \eta_0 y + \omega_0 t)\right] \quad \text{with} \quad k_0 \approx 10^{-28}\ \text{cm}^{-1}\ \text{sec}^{-3} \tag{55}$$

where the magnitude of k_0 follows from the expression

$$K = (K_x, K_y, K_z) \cong 3M\,\bar{\rho} g \frac{R_E^3 - 3zR_E^2}{r^3} \exp\left[i(\kappa_0 x + \eta_0 y + \omega_0 t)\right] \text{gm cm}^{-2}\ \text{sec}^{-2}$$

$$\cong 10^{-4}\ \text{gm sec}^{-2}\ \text{cm}^{-2} \tag{56}$$

with

M = mass of the moon, assuming the mass of the earth to be unity

r = distance between the center of the earth and the center of the moon

R_E = radius of the earth

For simplication, we take $\Gamma = \Gamma_0 = \text{constant}$, i.e., $\bar{\rho}(z) = \bar{\rho}_0 \exp(\Gamma_0 z)$. Now consider a rectangular basin

$$-L \leq x \leq +L, \qquad -B \leq y \leq +B, \qquad 0 \leq z \leq H$$

The tide-generating force (equation 55) is developed into a Fourier series with regard to the dimensions of the basin.

$$k_0 \exp\left[i\,(\kappa_0 x + \eta_0 y + \omega_0 t)\right]$$

$$= \sum_{\ell=-\infty}^{\infty} \sum_{m=-\infty}^{\infty} \hat{k}_{\ell,\,m} \exp\left[i\left(\frac{\ell\pi x}{L} + \frac{m\pi y}{B} + \omega_0 t \right)\right] \tag{57}$$

$$\ell = \pm 1, \ldots; \; m = \pm 1, \ldots$$

$$\hat{k}_{\ell,\,m} = \frac{k_0}{4LB} \int_{-L}^{L} \int_{-B}^{B} \exp i\pi \left(\frac{2L - \ell\lambda_0}{\lambda_0 L}\, x + \frac{2B - m\lambda'_0}{\lambda'_0 B}\, y \right) dx\,dy$$

Setting

$$\alpha_\ell = \frac{\pi(2L - \ell\lambda_0)}{\lambda_0}, \quad \beta_m = \frac{\pi(2B - m\lambda'_0)}{\lambda'_0} \tag{58}$$

we have after integration

$$\hat{k}_{\ell,\,m} = k_0 \frac{\sin\alpha_\ell}{\alpha_\ell} \frac{\sin\beta_m}{\beta_m} \tag{59}$$

and since by assumption λ_0 is not a multiple of $2L$, all $\hat{k}_{\ell,\,m}$ are not equal to zero.

The same expansion for $w(x,y,z,t)$ is

$$w(x, y, z, t) = \sum_{\ell=-\infty}^{\infty} \sum_{m=-\infty}^{\infty} W_{\ell,\,m}(z) \exp\left[i\left(\frac{\ell\pi x}{L} + \frac{m\pi y}{B} + \omega_0 t \right)\right] \tag{60}$$

and with

$$g\Gamma_0 \gg \omega_0^2, \; \Gamma_0 \frac{dW}{dz} \ll \frac{d^2W}{dz^2} \tag{61}$$

follows from equation 53

$$\frac{d^2 W_{\ell,\,m}}{dz^2} + \frac{g\Gamma_0\pi^2\left[\left(\frac{\ell}{L}\right)^2 + \left(\frac{m}{B}\right)^2\right] W_{\ell,\,m}}{\omega_0^2 - f^2} = \frac{\hat{k}_{\ell,\,m}}{\omega_0^2 - f^2} \tag{62}$$

$W_{\ell,\,m} = 0$ for $z = 0$ and $z = H$

The solution of (62) is

$$W_{\ell,m}(z) = \frac{\hat{k}_{\ell,m}}{g\Gamma_0\pi^2\left[\left(\frac{\ell}{L}\right)^2+\left(\frac{m}{B}\right)^2\right]}\left\{1-\cos\left[\frac{g\Gamma_0\left[\left(\frac{\ell}{L}\right)^2+\left(\frac{m}{B}\right)^2\right]}{\omega_0^2-f^2}\right]^{1/2}\pi z\right.$$

$$+\left.\frac{\cos\left[\frac{g\Gamma_0\left[\left(\frac{\ell}{L}\right)^2+\left(\frac{m}{B}\right)^2\right]}{\omega_0^2-f^2}\right]^{1/2}\pi H-1}{\sin\left[\frac{g\Gamma_0\left[\left(\frac{\ell}{L}\right)^2+\left(\frac{m}{B}\right)^2\right]}{\omega_0^2-f^2}\right]^{1/2}\pi H}\sin\left[\frac{g\Gamma_0\left[\left(\frac{\ell}{L}\right)^2+\left(\frac{m}{B}\right)^2\right]}{\omega_0^2-f^2}\right]^{1/2}\pi z\right\} \quad (63)$$

The amplitude factor

$$\frac{\hat{k}_{\ell,m}}{g\Gamma_0\pi^2\left[\left(\frac{\ell}{L}\right)^2+\left(\frac{m}{B}\right)^2\right]}$$

with

$$\hat{k}_{\ell,m} \cong 10^{-28}\ \mathrm{cm^{-1}\ sec^{-3}},\quad g\Gamma_0 \cong 10^{-4}\ \mathrm{sec^{-2}},\quad \ell = m = 1$$

$$L = B \cong 10{,}000\ \mathrm{km}$$

has the magnitude $10^{-8}\ \mathrm{cm\ sec^{-1}}$ from which an amplitude of 10^{-3} results for ζ. Therefore the amplitudes of the first and second terms in the brackets are negligible. The third contains a resonance factor.

For any combination of wavelength which fulfills the condition

$$\left(\frac{\ell}{L}\right)^2+\left(\frac{m}{B}\right)^2 = \frac{(2n-1)^2(\omega_0^2-f^2)}{g\Gamma_0 H^2},\quad n = \pm1, \pm2, \ldots, \quad (64)$$

it follows that $W_{\ell,m} \to -\infty$. Introducing friction, we get finite amplitudes. It can be shown that the amplitudes ζ are of the magnitude 10 meters. Two cases are distinguished:

(1) The case where angular frequency of internal waves is greater than Coriolis parameter, i.e., $\omega_0^2 > f^2$

Because the right-hand side of (64) is positive, the condition is fulfilled if (a) ℓ and m are real (waves with finite crests); (b) $\ell = 0$ or $m = 0$, the conditions for waves with infinite crests; or (c) $m = im^*$, ℓ real and $(\ell/L)^2 > (m/B)^2$ which are Kelvin waves which travel in the x direction. The supposition for these cases is that the tide-generating force is expandable in terms of L and B.

(2) The case where angular frequency of internal waves is less than Coriolis parameter, i.e.,

$$\omega_0^2 < f^2$$

Because of the negative sign on the right-hand side, equation 64 can be fulfilled only with $m = im^*$ and $(\ell/L)^2 < (m/B)^2$ These are Kelvin waves. Under the supposition that the tide-generating force can be expanded into a series of Kelvin waves, internal tidal waves of the Kelvin type with infinitely high amplitudes are possible in all areas where $\omega_0^2 < f^2$. They are really no longer of the Kelvin type since, because of the resonance factor, the amplitude is infinite everywhere in the frictionless case. They are, therefore, identical with internal waves with infinitely long crests.

The condition in equation 64 is identical with the characteristic equation of free internal waves for the odd modes, which are always in phase with the corresponding harmonics of the tide-generating force (harmonics in regard to the ocean basin). To the extent that the surface tides can be considered to be forced waves, the direction in which the internal tides travel should correspond with that of the surface tides.

Considering the Pacific Ocean, we should expect semidiurnal waves in the entire ocean corresponding to the expansion of the force and, therefore, to the surface M_2-tide. The diurnal internal wave is influenced by $\phi = 28^\circ$ or $\phi = 30^\circ$, where $\omega_0 = f$ for the K_1 – or 0_1 – tide. North of these latitudes, the internal wave should have infinitely long crests and travel parallel to the coast. South of the latitude $\omega_0 = f$, the internal tidal waves should travel in about the same direction as the surface waves.

Free Diurnal Internal Tidal Waves at 30° N

To determine whether diurnal internal waves in the ocean are mainly forced or free waves, we may carry out observations near 30°N. In contrast to the forced internal waves mentioned in the preceding section, free internal tidal waves of the diurnal period can occur only in the area $\omega_0 > f$, that is, south of 30°N for the K_1 –tide and south of 28°N for the 0_1 –tide. The behavior of free waves in the entire area where $\omega \geq f$ in the case of a variable Coriolis parameter is given below.

Suppose $f = f(y)$ and waves $\psi(x,y,z,t) = \overset{\circ}{\psi}(x,y,z)$ exp $(i\omega t)$. Then the following equations describe free internal waves:

$$i\omega \overset{\circ}{u} + f \overset{\circ}{v} + \frac{\partial P}{\partial x} = 0 \tag{65}$$

$$i\omega \overset{\circ}{v} - f \overset{\circ}{u} + \frac{\partial P}{\partial y} = 0 \tag{66}$$

$$i\omega \overset{\circ}{w} - g\overset{\circ}{R} + \frac{\partial \overset{\circ}{P}}{\partial z} + \Gamma \overset{\circ}{P} = 0 \tag{67}$$

$$i\omega \overset{\circ}{R} + \Gamma \overset{\circ}{w} = 0 \tag{68}$$

$$\frac{\partial \overset{\circ}{u}}{\partial x} + \frac{\partial \overset{\circ}{v}}{\partial y} + \frac{\partial \overset{\circ}{w}}{\partial z} = 0 \tag{69}$$

Elimination of $\overset{\circ}{u}$, $\overset{\circ}{v}$, $\overset{\circ}{w}$, and $\overset{\circ}{R}$ yields

$$\frac{\partial^2 \overset{\circ}{P}}{\partial x^2} + \frac{\partial^2 \overset{\circ}{P}}{\partial y^2} - \frac{\omega^2 - f^2}{g\Gamma - \omega^2} \frac{\partial^2 \overset{\circ}{P}}{\partial z^2} - \frac{if'(\omega^2 + f^2)}{\omega(\omega^2 - f^2)} \frac{\partial \overset{\circ}{P}}{\partial x} + \frac{2ff'}{\omega^2 - f^2} \frac{\partial \overset{\circ}{P}}{\partial y}$$

$$- \frac{\omega^2 - f^2}{g\Gamma - \omega^2} \left(\Gamma - \frac{g\Gamma'}{g\Gamma - \omega^2} \right) \frac{\partial \overset{\circ}{P}}{\partial z} + \frac{\omega^2 - f^2}{(g\Gamma - \omega^2)^2} \omega^2 \Gamma' \overset{\circ}{P} = 0 \tag{70}$$

where $f' = \frac{df}{dy}$ and $\Gamma' = \frac{d\Gamma}{dz}$

We now consider waves with infinitely long crests, $\frac{\partial}{\partial x} = 0$, and neglect the small terms $\frac{g}{g\Gamma - \omega^2} \frac{\partial}{\partial z} << 1$. It follows that

$$\frac{1}{\omega^2 - f^2} \left\{ \frac{\partial^2 \overset{\circ}{P}}{\partial y^2} + \frac{2ff'}{\omega^2 - f^2} \frac{\partial \overset{\circ}{P}}{\partial y} \right\} - \frac{1}{g\Gamma - \omega^2} \left\{ \frac{\partial^2 \overset{\circ}{P}}{\partial z^2} + \Gamma \frac{\partial \overset{\circ}{P}}{\partial z} \right.$$

$$\left. - \frac{\omega^2 \Gamma'}{g\Gamma - \omega^2} \overset{\circ}{P} \right\} = 0 \tag{71}$$

with a separation

$$\overset{\circ}{P}(y, z) = \tilde{G}(y) \hat{P}(z) \tag{72}$$

yields

$$\frac{d^2 \tilde{G}}{dy^2} + \frac{2ff'}{\omega^2 - f^2} \frac{d\tilde{G}}{dy} + \epsilon(\omega^2 - f^2) \tilde{G} = 0 \tag{73}$$

$$\frac{d^2 \hat{P}}{dz^2} + \Gamma \frac{d\hat{P}}{dz} + \left[(g\Gamma - \omega^2)\epsilon - \frac{\omega^2 \Gamma'}{g\Gamma - \omega^2} \right] \hat{P} = 0 \tag{74}$$

After differentiation of (74) under consideration of (67), (68), and $-\frac{g}{g\Gamma - \omega^2} \frac{\partial}{\partial z} << 1$, it follows that

$$\frac{d^2 W}{dz^2} + \Gamma \frac{dW}{dz} + (g\Gamma - \omega^2)\epsilon W = 0 \tag{75}$$

Therefore, equation 73 can be interpreted as the y–dependency of W.

Equation 73 may be written in the form

$$\frac{d}{dy}\left(\frac{1}{\omega^2 - f^2}\ \frac{d\tilde{G}}{dy}\right) + \epsilon\ \tilde{G} = 0 \tag{76}$$

We choose the origin of the coordinate system so that $y = y_0$ is located at $f = 0$ (equator) and $y = y_1$ at $f = \omega$. With the transformations

$$Y = \frac{1}{(\omega^2 - f^2)^{1/4}}\ \tilde{G}, \qquad \xi = \frac{1}{j}\int_0^y (\omega^2 - y^2)^{1/2}\, dy,$$

$$j = \frac{1}{\pi}\int_{y_0}^{y_1} (\omega^2 - f^2)^{1/2}\, dy \tag{77}$$

for the area $\omega \geq f$ we get from (75) the Schrodinger equation

$$\frac{d^2Y}{d\xi^2} + [\,K^2 - \Upsilon(\xi)\,]\,Y = 0 \tag{78}$$

with

$$K^2 = j^2\epsilon \tag{79}$$

and

$$\Upsilon = (\omega^2 - f^2)^{1/4}\ \frac{d^2}{d\xi^2}\left\{\frac{1}{(\omega^2 - f^2)^{1/4}}\right\} = \frac{j^2}{2}\left\{\frac{ff'' + f'^2}{(\omega^2 - f^2)^2} + \frac{7}{2}\ \frac{(ff')^2}{(\omega^2 - f^2)^3}\right\} \tag{80}$$

Because of the smallness of f' and f'', $\Upsilon(\xi)$ is negligible in regard to K^2 for all areas outside of ξ, where $\omega = f(\xi)$. Therefore, we suppose $\Upsilon(\xi) = 0$ for these regions and get

$$Y(\xi) = Y_0 \exp\,(ik\xi),\ \omega > f \tag{81}$$

or

$$\tilde{G}(y) = G_0\ (\omega^2 - f^2)^{1/4} \exp\left[i\epsilon^{1/2}\int_0^y [\omega^2 - f^2(y)]^{1/2} dy\right] \tag{82}$$

In order to find the influence of the singularity at ξ, we consider (78) to be an inhomogenous equation

$$\frac{d^2Y}{d\xi^2} + K^2Y = \Upsilon(\xi)\,Y \tag{83}$$

with the solution

$$Y(\xi) = Y(0)\cos\ k\xi + \frac{Y'(0)}{k}\sin\ k\xi + \frac{1}{k}\int_0^{\xi} \sin\ k\,(\xi - \xi^*)\ \Upsilon(\xi^*)\ Y(\xi^*)\, d\xi^* \tag{84}$$

Υ has the character of a δ -function:

$$\Upsilon(\xi) = \delta(\xi - \xi_1),\ \xi_1 = \frac{1}{j}\int_0^{y_1} [\omega^2 - f^2(y)]^{1/2}\, dy,\ \omega^2 \cong f^2(y_1) \qquad (85)$$

Therefore, equation 84 can be solved:

$$Y(\xi) = Y(0)\cos k\xi + \frac{Y'(0)}{k}\sin k\xi + \frac{Y(\xi_1)}{k}\sin k(\xi - \xi_1) \qquad (86)$$

This solution shows that at $\xi = \xi_1$, given by $\omega = f$, a reflected wave is created which travels back into the area $\omega > f$, having the amplitude $\frac{Y(\xi)}{k}$, the wave number k, and the phase $k\xi_1$. Because of $\tilde{G} = (\omega^2 - f^2)Y$, the vertical component $w = \tilde{G}(y)\ W(z)$ of the wave vanishes at $\omega = f$. In the following section it is shown that the spectra of the chain records do not indicate any significant decrease of the amplitudes of the diurnal internal tidal wave at $\phi = 30°$ or north of it. Therefore, it is believed that the observed internal tidal waves are forced waves.

ANALYSIS AND INTERPRETATION OF THERMISTOR CHAIN DATA RECORDED AT A DRIFT STATION

As pointed out previously, an advantage of anchor stations is that their data can be interpreted directly by the theory of internal waves. They permit the easiest computation of the amplitudes of the modes.

Drift Station 1

At Drift Station 1, a continous temperature-depth recording was made with the NEL thermistor chain by USS MARYSVILLE from 2135 hours on 10 October to 2135 hours on 11 October 1963 at the central position 31°00′N, 121°00′W. The ship was drifting approximately 1 knot to the southeast, which might have caused a doppler shift in the higher modes. Numerical computations of density are based on a hydrographic station in the nearby area. These data are given in table 1.

A Fourier analysis has been made on the depth fluctuations of the isotherms. The spectrum of the mean value for all isotherms is shown in figure 5. Both the diurnal and semidiurnal internal tidal waves have amplitudes of about 6 meters (mean value for the upper 200 meters). They are, therefore, equally important.

In order to analyze the contributions of each mode to the resultant amplitudes, the vertical change of the amplitudes must be decomposed into the modes. This was not done because the chain is only 900 feet long and therefore, the observations did not extend to the bottom.

Table 1. HYDROGRAPHIC DATA FOR STATION 1

Date: 9 October 1963. Position: 30°07′N, 120°10′W. Depth: 3800 meters.

Depth (m)	Temp. (°C)	Salinity (‰)	σ_t	Accepted $\frac{1}{\bar{\rho}} \frac{d\bar{\rho}}{dz} \cdot 10^{-6}$
0	21.42	33.72	23.43	0.21
10	21.40	33.68	24.40	0.22
20	21.31	33.68	23.42	4.68
30	21.20	33.73	23.50	9.50
50	16.50	33.71	24.66	27.58
75	13.67	33.69	25.27	19.57
100	11.59	33.69	25.58	12.27
150	9.60	33.74	26.04	4.90
200	8.92	34.05	26.40	6.23
300	8.71	34.34	26.67	0.64
400	7.49	34.31	26.82	2.10
500	6.15	34.26	26.95	2.18
600	5.53	34.39	27.17	1.12
800	4.66	34.45	27.30	0.98
1000	3.93	34.59	27.48	0.76
1200	3.38	34.66	27.58	0.48
1500	2.71	34.69	27.65	0.24
2000	2.15	34.71	27.70	0.10

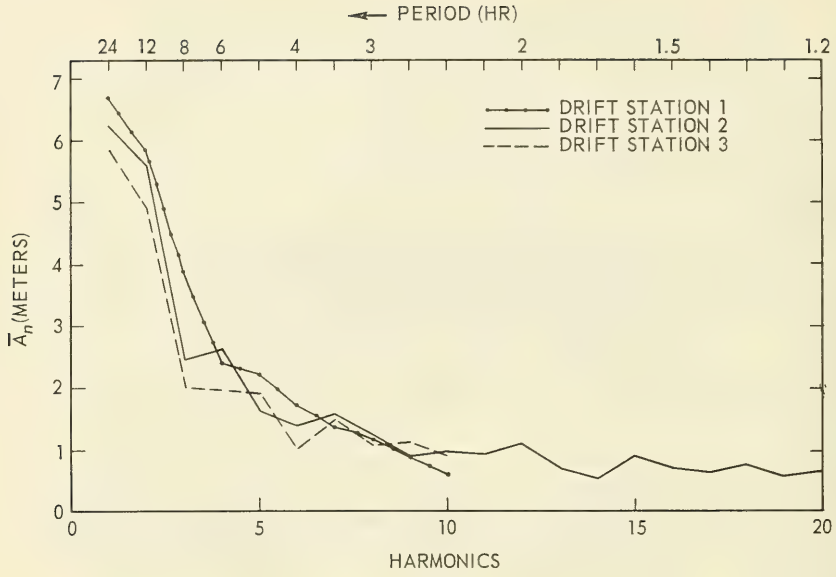

Figure 5. Mean amplitude spectrum for the upper 180 meters at Drift Stations 1, 2, and 3.

Drift Stations 2 and 3

In October 1963, USS MARYSVILLE studied the situation closer to the coast by making measurements with the thermistor chain at Drift Stations 2 and 3, near Sixty Mile Bank. Each observation was 24 hours long (2145 hours to 2130 hours, 15-16 October; 2345 to 2330, 16-17 October). In the first measurement the drift was about 15 miles in 24 hours (approximately 32 cm/sec); in the second, drift was negligible. Doppler shifting appeared to be very small in the tidal range. Representative hydrographic data for both stations are given in table 2.

Each isotherm was subjected to a harmonic analysis. Their mean depths were 32, 40, 45, 49, 56, 76, 102, 142, and 173 meters. The sampling rate was every 15 minutes. Mean values of the computed amplitudes, $\bar{A}_n$, are shown in figure 5 as a function of the harmonics (lower scale) or the periods (upper scale). It can be seen from these curves that the tidal periods govern the spectrum. We get mean amplitudes, $\bar{A}_n$, of about 6 meters for both the diurnal and semidiurnal internal tides in the upper 180 meters, and this is in good agreement with station 1. For comparison, figure 6 shows the predicted tidal curve at San Diego, California, from 10 to 17 October 1963. The tides are mainly diurnal at the beginning and strongly semidiurnal at the end of the period. It therefore seems reasonable to expect internal tides of both periods to be present at all times,

Table 2. HYDROGRAPHIC DATA FOR STATIONS 2 AND 3

Date: 18 October 1963. Position: 32°15′N, 118°20′W. Depth: 1692 meters.

Depth (m)	Temp. (°C)	Salinity (‰)	σ_t	Accepted $\frac{1}{\bar{\rho}} \frac{d\bar{\rho}}{dz} \cdot 10^{-6}$
0	20.57	33.57	23.54	0.10
10	20.45	33.56	23.56	1.29
20	20.25	33.55	23.61	1.79
30	20.05	33.54	23.66	10.43
50	13.50	33.55	25.18	20.78
75	12.18	33.62	25.50	8.66
100	11.38	33.72	25.80	4.88
150	10.30	34.06	26.18	6.48
200	9.14	34.12	26.42	3.21
300	7.57	34.07	26.63	2.19
400	6.97	34.18	26.81	1.57
500	6.24	34.27	26.96	1.81
600	5.66	34.38	27.11	1.43
800	4.77	34.42	27.25	0.39
1000	4.66	34.41	27.27	0.20

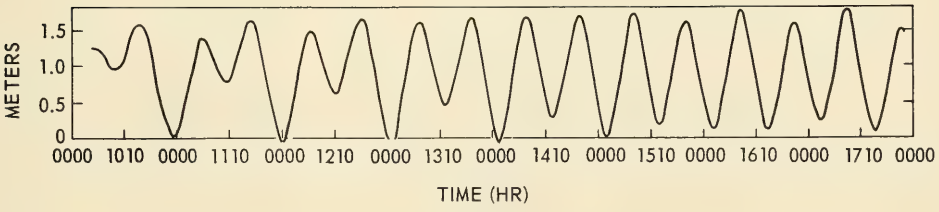

Figure 6. Predicted tides at San Diego, California, for the period 10 Oct 63 - 17 Oct 63.

because they are less influenced by damping. The intensity in the tidal range is about $35 m^2$ (approximately 380 ft^2)/harmonic.

The eigenfunctions, $W_n(z)$, have been computed using the values of $\frac{1}{\bar{\rho}} \frac{d\bar{\rho}}{dz}$ given in table 2. They are shown for the upper 500 meters in figures 7A and B. The eigenvalues, ϵ for $n = 1$ to $n = 11$, and the corresponding phase velocities, c_n according to the approximate formula given in equation 10, are listed below.

Eigenvalues (m^{-1} sec^2)

ϵ_1 = 0.4258	ϵ_5 = 12.6506	ϵ_9 = 45.9762
ϵ_2 = 1.6454	ϵ_6 = 20.2472	ϵ_{10} = 57.4772
ϵ_3 = 4.2178	ϵ_7 = 27.3472	ϵ_{11} = 70.0884
ϵ_4 = 7.4234	ϵ_8 = 36.0545	

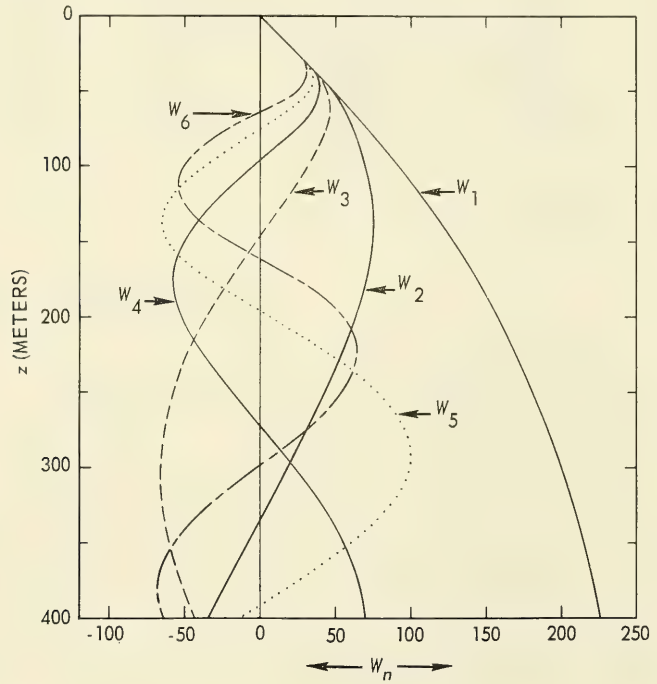

A. MODES 1-6

Figure 7. Representative eigenfunctions $W_n(z)$ for the upper 500 meters for Drift Stations 2 and 3.

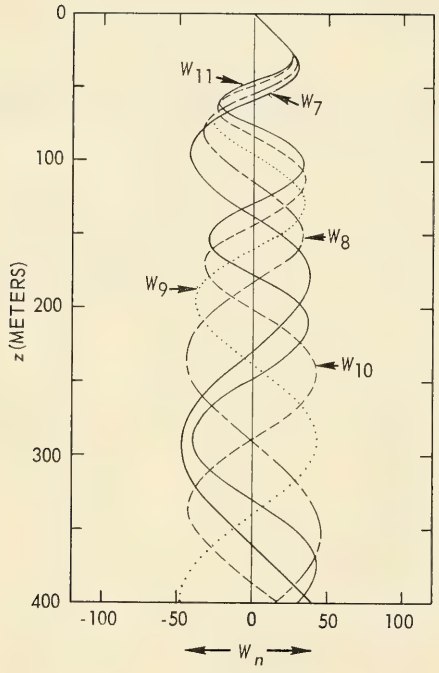

B. MODES 7-11

Figure 7 (continued).

Phase Velocity (m sec^{-1})

c_1 = 4.80	c_5 = 0.88	c_9 = 0.46
c_2 = 2.44	c_6 = 0.70	c_{10} = 0.41
c_3 = 1.52	c_7 = 0.60	c_{11} = 0.37
c_4 = 1.15	c_8 = 0.53	

Anchor Station 4

After observations at the drift stations, similar measurements were made at an anchored station. The hydrographic data obtained are listed in table 3.

Table 3. HYDROGRAPHIC DATA FOR STATION 4

Date: 3 December 1963. Position: 32°04′N, 118°30′W. Depth: 330 meters.

Depth (m)	Temp. (°C)	Salinity (‰)	σ_t	Accepted $\frac{1}{\bar{\rho}} \frac{d\bar{\rho}}{dz} \cdot 10^{-6}$
0	17.41	33.18	24.50	0.00
10	17.41	33.60	24.38	0.62
20	17.41	33.64	24.40	14.95
30	17.38	33.75	24.50	14.95
50	13.40	33.44	25.13	13.66
75	12.04	33.59	25.51	11.77
100	10.68	33.72	25.86	6.47
150	9.67	33.92	26.19	4.00
200	8.60	33.96	26.39	4.51
250	7.94	34.13	26.63	2.29
300	7.68	34.13	26.65	0.67

Chain records were obtained for Anchor Station 4 for the period from 0500 to 2400 hours on 3 December 1963. Fourier analysis of the 12-hour and 24-hour harmonics produced the results given in table 4. The mean rms amplitudes for the upper 200 meters are 4.0 meters and 9.4 meters for the diurnal and semidiurnal internal tides, respectively.

Because of the shallowness of the station, records are available for the entire upper half of the water. Therefore, it seems to be possible to compute the contributions of the first to fourth modes to the observed amplitudes.

Figures 8 A and B show the eigenfunction distribution for the first through eleventh modes. The contributions of these modes were computed by using equation 19. The 17°, 13°, 11°, and 9° isotherms were used for these computations. The results for the first four modes are summarized in table 5. Generally the second mode has much more influence than the other ones. This computation is not exact because the measurements are not spaced over the entire water column.

Table 4. AMPLITUDES OF THE FLUCTUATIONS WITH DIURNAL AND SEMIDIURNAL PERIODS AT STATION 4

Isotherm	Mean Depth	Diurnal Period Fourier Amplitudes			Semidiurnal Periods Fourier Amplitudes		
(°C)	a_0	a	b	A	a	b	A
17	32.0	2.9	2.9	4.2	0.3	-5.9	5.9
16	40.0	3.8	2.4	4.5	-1.1	-6.3	6.3
15	44.6	3.5	2.8	4.5	-2.0	-7.0	7.4
13	56.6	4.8	2.8	5.6	-0.4	-8.0	8.0
12	76.4	-1.9	1.8	2.6	1.5	-5.5	5.7
11	101.9	0.0	2.8	2.8	10.2	-1.4	9.7
10	142.3	-2.2	-3.0	3.8	11.2	10.7	15.4
9	173.0	-3.8	-0.1	3.8	8.7	14.4	16.9

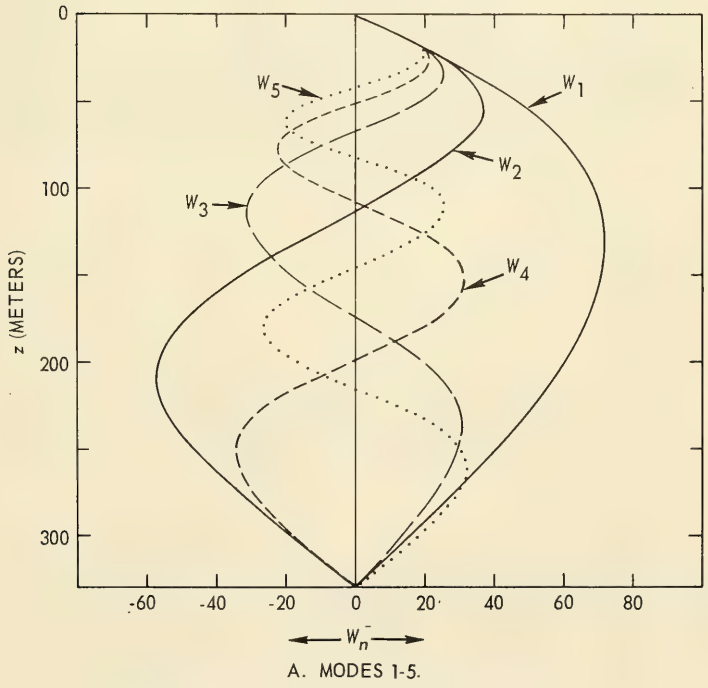

Figure 8. Eigenfunctions $W_n(z)$ at Anchor Station 4, modes 1 - 9.

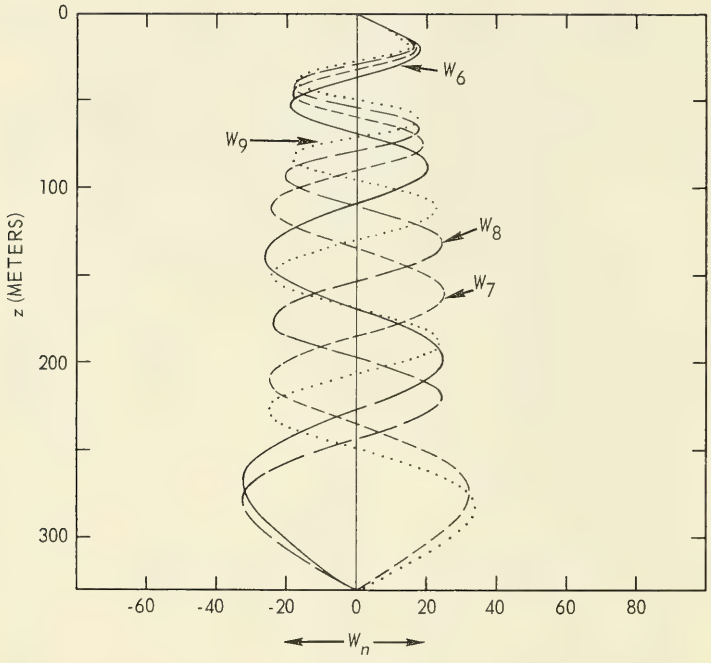

B. MODES 6-9.

Figure 8 (continued).

Table 5. CONTRIBUTIONS OF FIRST FOUR MODES TO THE OBSERVED FLUCTUATIONS WITH DIURNAL PERIODS AT STATION 4.

Depth (m)	A_1W_1	A_2W_2	A_3W_3	A_4W_4	$\sum_n A_nW_n$	a	B_1W_1	B_2W_2	B_3W_3	B_4W_4	$\sum_n B_nW_n$	b
32.0	0.6	1.8	2.0	-1.5	2.9	2.9	0.8	1.8	-0.7	1.0	2.9	3.0
56.6	0.9	2.2	1.0	0.5	4.6	4.6	1.3	2.2	-0.3	-0.4	2.8	2.9
101.9	1.2	0.6	-2.3	0.5	0.0	-0.0	1.8	0.6	0.8	-0.3	2.9	2.8
173.0	1.2	-2.9	-0.1	-1.8	-3.6	-3.7	1.8	-2.9	0.0	1.2	0.1	0.1

Analysis of Internal Tides from a Cross-Like Section

To obtain preliminary information on the direction of progress of the internal tides, the thermistor chain was towed in a cross-shaped pattern moving, consecutively, from west to east, east to west, north to south, and south to north. The end points of the cross were 31°54′N, 119°25′W; 31°54′N, 117°10′W; 32°50′N, 118°16′W; and 30°52′N, 118°16′W. The duration of each leg was about 20 hours. Mean water depth was about 1600 meters. As shown by the spectra at the drift stations, the energy is peaked in the tidal range; therefore, even with these short records, dominant energy shift over frequency came mainly from the tidal peaks.

Figures 9 and 10 show the amplitude spectra for the four legs. Because the records are short, high confidence cannot be expected. The spectra were obtained at trial periods lasting from 2 hours to 38 hours. The amplitudes in the periods longer than 12 hours are generally larger in the case of the west-east and the south-north legs than in the other two legs. If their spectral densities are compared at common frequencies, they would imply that the semidiurnal, as well as the diurnal internal tidal waves run in a northeasterly direction. This supports the results obtained by H.Sumners and K.O. Emery.[7] The additional maximum in the east-west and north-south directions in periods near 8 hours might be a reflected wave traveling in a southwesterly direction and having a smaller amplitude than the waves traveling to the northeast. Because the amplitudes are different, we cannot expect standing internal tidal waves in the Gulf of Santa Catalina. In agreement with the results presented on pages 15–20, the energy level is higher in the towed records than in the records from the drift stations.

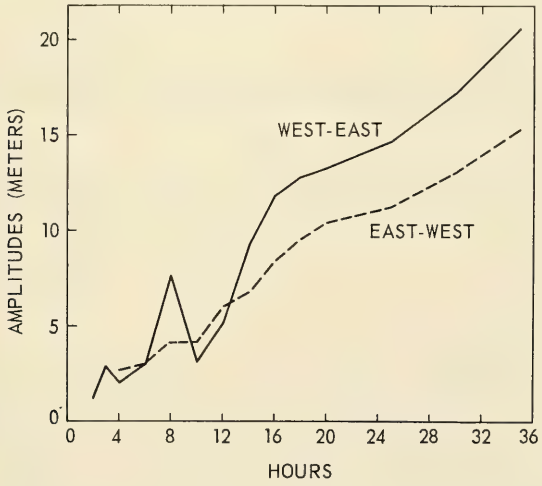

Figure 9. Amplitude spectrum for the legs east-west and west-east.

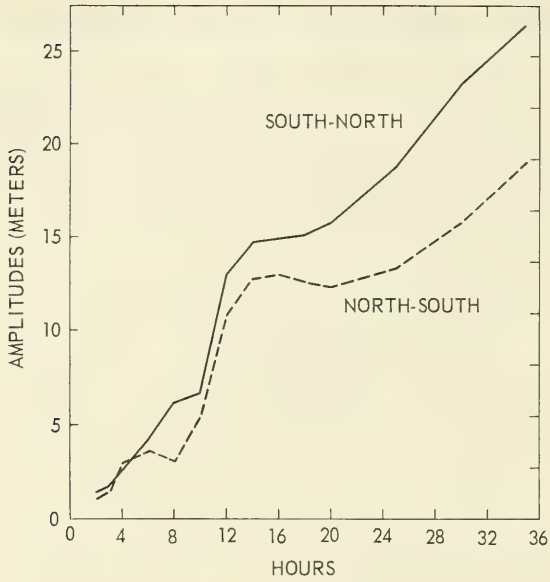

Figure 10. Amplitude spectrum for the legs north-south and south-north.

ANALYSIS OF CHAIN DATA FROM SAN DIEGO TO HAWAII

In August 1961, USS MARYSVILLE went from San Diego, California to Honolulu, Hawaii (by the route shown in fig. 11) and recorded temperature distributions in the upper 230 meters with the thermistor chain. The ship's mean direction was about 255°; mean speed was 6 knots. The data obtained during the cruise were reported fully in reference 11, in which short-period waves of encounter were analyzed for slope and power spectrum. Here, the longer internal tide is given primary consideration. The record selected for the analysis covers the period from 2000 hours on 4 August to 2000 on 17 August.

The record was processed as follows:

1. Data from one day's isotherms form one set. A 24-hour record corresponds to about 150 nautical miles.

2. The depths of the isotherms were read from the analog record every 10 minutes, taking mean values (by sight) for these points.

3. The Fourier analysis was carried out using three consecutive sets. The combined sets are overlapping: 1-3, 2-4, 10-12, 11-13. It is assumed that the spectra represent the situation in the centers of these areas. Fourier components

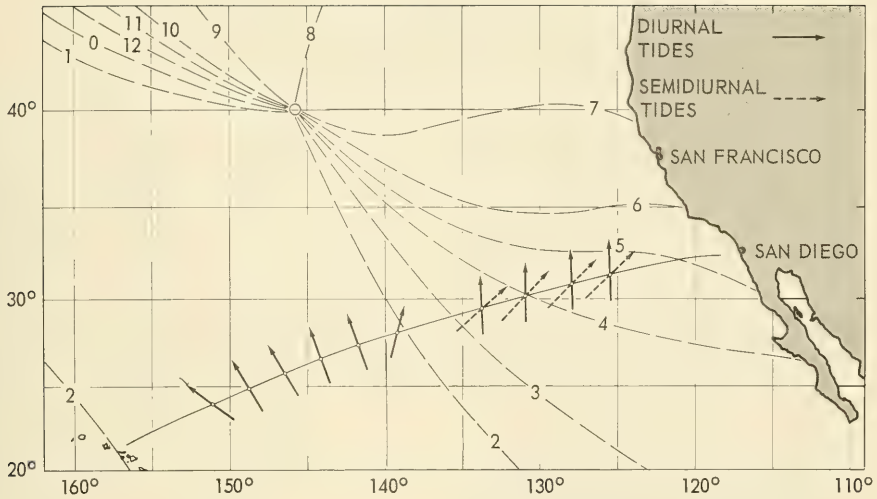

Figure 11. Cotidal lines of the semidiurnal tides (after Dietrich, ref. 13) and direction of progress of the internal semidiurnal and diurnal tidal waves on the cruise from San Diego to Hawaii.

were computed for each isotherm up to the 40th harmonic. The corresponding periods are $72/n$ hours.

4. To check the influence of the mean inclination of the isotherms on the spectra, the depth change of the isotherms was computed by taking the difference of the mean values of the first and last 10 hours of each 72-hour record.

5. Mean values, $\overline{A}_n$, for all isotherms of each combined set were computed from the A_n.

As is well known from hydrographic sections,[12] the stationary isotherms are inclined in the upper 1000 meters, increasing in depth toward the west. If the linear depth change of an isotherm over a length L is denoted by Δ and the Fourier amplitudes of this interval are denoted by $a_{n,st}$ and $b_{n,st}$, then Fourier analysis leads to the amplitude spectrum

$$A_{n,st} = \frac{\Delta}{n\pi}, \text{ where } A_{n,st} = [a_{n,st}{}^2 + b_{n,st}{}^2]^{1/2} \text{ and } a_n = 0,\ b_n = \frac{\Delta}{n\pi} \text{ with } n = 1,2,\ldots$$

Any Fourier analysis of the chain records considered here is therefore strongly influenced in the long-period range by this stationary inclination. The amplitudes, A_n, of the periodic changes are superimposed on this hyberbolic spectrum of the stationary component of the isotherm.

Table 6 gives the mean depth change, $\overline{\Delta}$, of the isotherms for each combined set, the expected amplitude, $\overline{A}_{0,st} = \frac{\overline{\Delta}}{\pi}$ due to these changes, $\overline{\Delta}$, and the analyzed amplitudes, $\overline{A}$, from the record. The numbers show that $\overline{A}$ results mainly from the stationary inclination of the isotherms.

Table 6. STATIONARY DEPTH CHANGE $\overline{\Delta}$ OF THE ISOTHERMS IN THE UPPER 230 METERS, ITS FOURIER AMPLITUDE $\overline{A}_{o,st}$ AND THE ANALYZED AMPLITUDE $\overline{A}_o$ OF THE RECORD

Set	$\overline{\Delta}$	$\overline{A}_{o,st}$	$\overline{A}_o$
1-3	54.1	17.3	22.4
2-4	86.2	27.5	35.3
3-5	56.6	18.1	28.7
4-6	20.7	6.6	8.7
6-8	25.6	8.2	16.3
7-9	17.1	5.4	11.5
8-10	25.3	8.0	20.0
9-11	45.0	14.4	16.2
10-12	2.1	0.7	2.1
11-13	35.4	11.3	16.2

DISCUSSION OF RESULTS

Figures 12-21 show the analyzed amplitudes $\overline{A}_n$. The dashed line represents the supposed stationary amplitude distribution due to the inclination of the isotherms. The general shape of the dashed line intersecting the minimum values agrees approximately with a function that is propotional to $1/n$.

In order to determine the doppler shifts one must know the phase velocity, c, and the direction of the internal waves. Since a hydrographic station was not available for the time, the density distribution from STRANGER station 95 ($\phi = 30°20.5'$ N, $\lambda = 119°27'$ W; depth, 3840 m) was substituted.

The phase velocities for the 1-4 modes are :

$c_1 = 2.19$ msec^{-1}, $c_2 = 1.20$ msec^{-1},

$c_3 = 0.59$ msec^{-1}, $c_4 = 0.47$ msec^{-1}.

Because the actual phase velocities in August 1961 may differ from these values, it is not possible to attribute the higher modes to the peaks of the computed spectra.

The rules from which the direction of the internal tidal waves were determined are demonstrated in figure 12. Here, one group of peaks appears in the range between 24 hours and 7.2 hours, another beyond 5.5 hours. It is known from the drift stations that the diurnal and semidiurnal tides are dominant in the area under consideration. For this reason the first group of peaks are identified as the modes of the diurnal internal tides. The first mode is thus assumed to appear at 18 hours, having been shifted from 25 hours. Using equation 26, phase velocity $c_1 = 2.19$ m/sec^{-1} corresponding to the first mode, and ship velocity

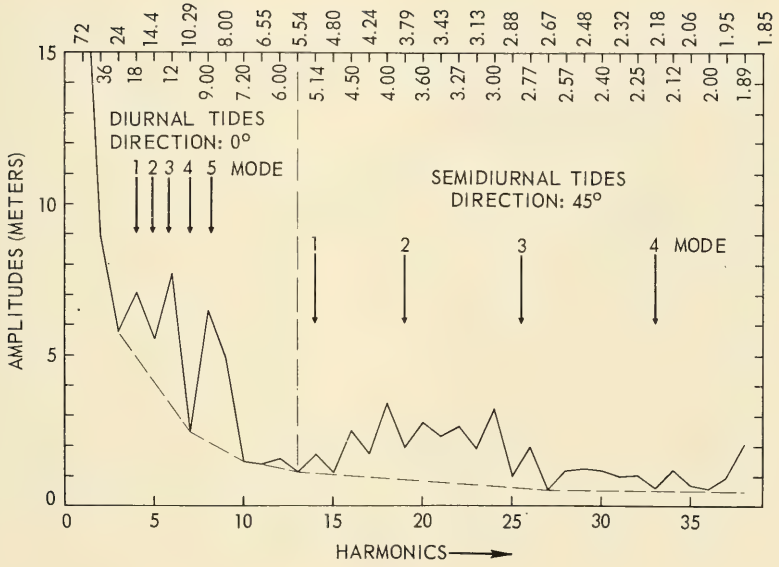

Figure 12. Mean amplitudes $\bar{A}_n$ for the upper 200 meters, San Diego-Honolulu. Set 1-3, 4 Aug 61, 2000 - 7 Aug 61, 2000.

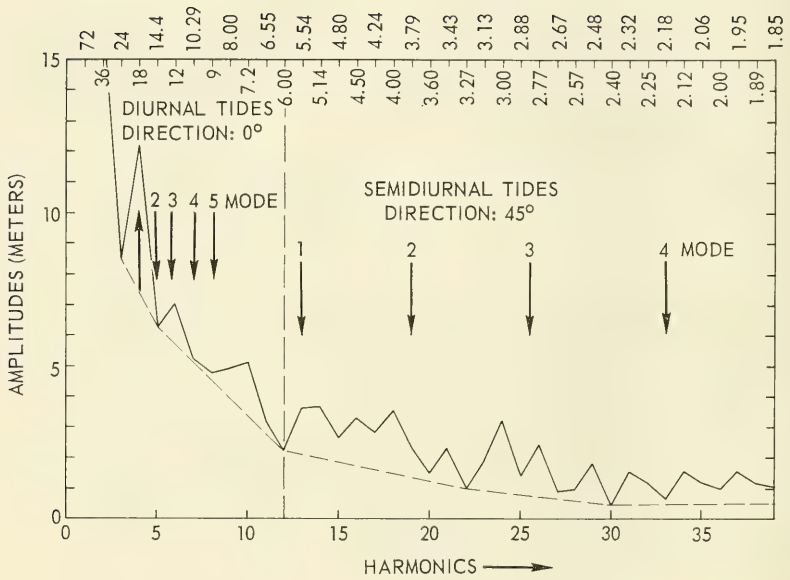

Figure 13. Mean amplitudes $\overline{A}_n$ for the upper 200 meters, San Diego-Honolulu. Set 2-4, 5 Aug 61, 2000 - 8 Aug 61, 2000.

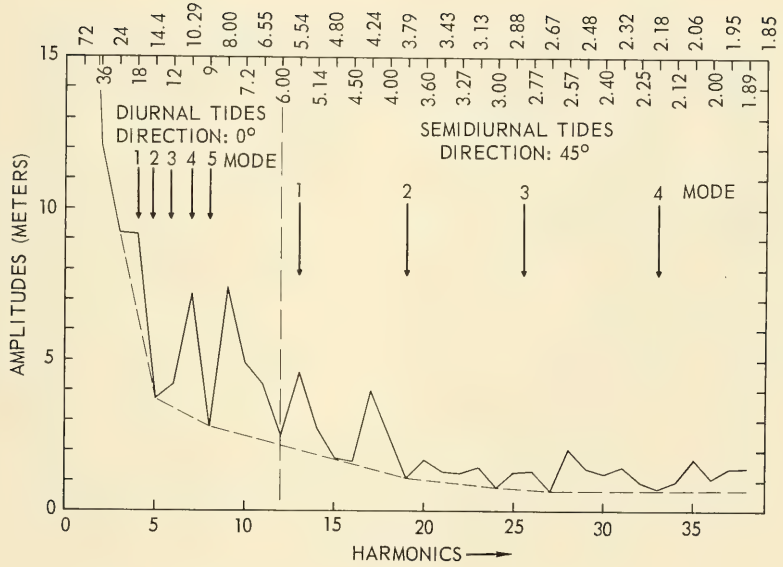

Figure 14. Mean amplitudes $\overline{A}_n$ for the upper 200 meters, San Diego-Honolulu. Set 3-5, 6 Aug 61, 2000 - 9 Aug 61, 2000.

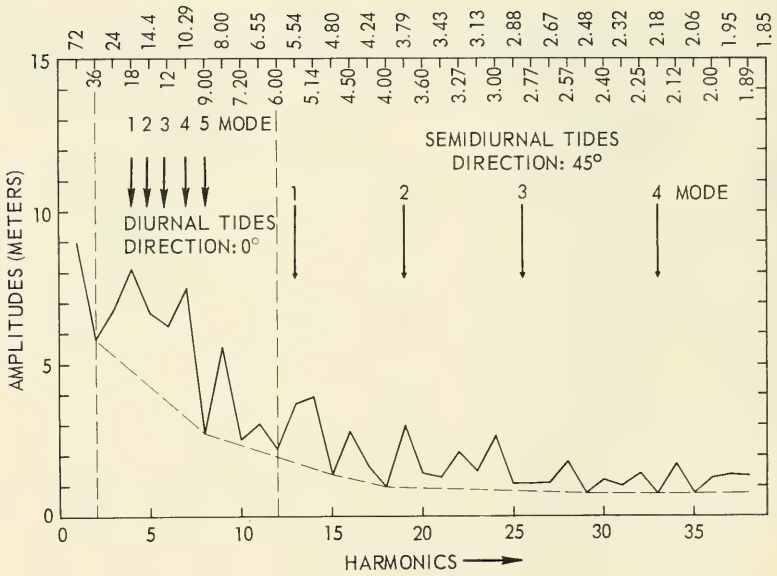

Figure 15. Mean amplitudes $\bar{A}_n$ for the upper 200 meters, San Diego- Honolulu. Set 4-6, 7 Aug 61, 2000 - 10 Aug 61, 2000.

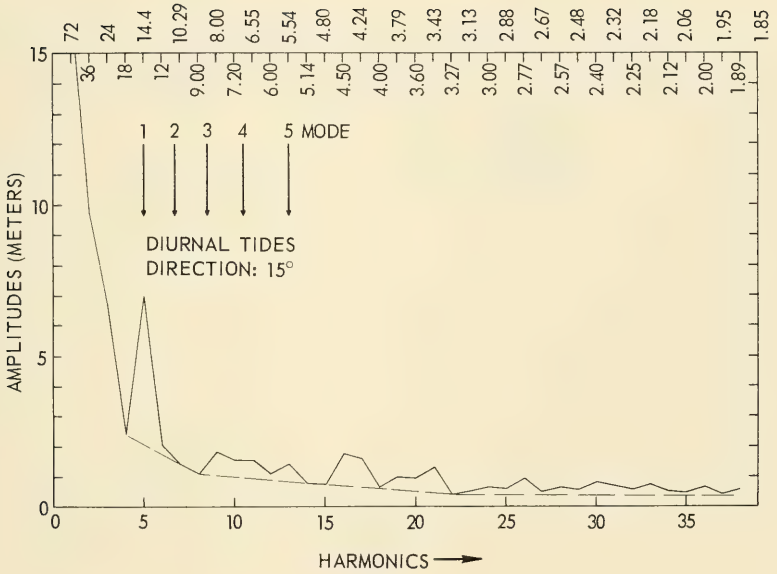

Figure 16. Mean amplitudes $\bar{A}_n$ for the upper 200 meters, San Diego-Honolulu. Set 6-8, 9 Aug 61, 2000 - 12 Aug 61, 2000.

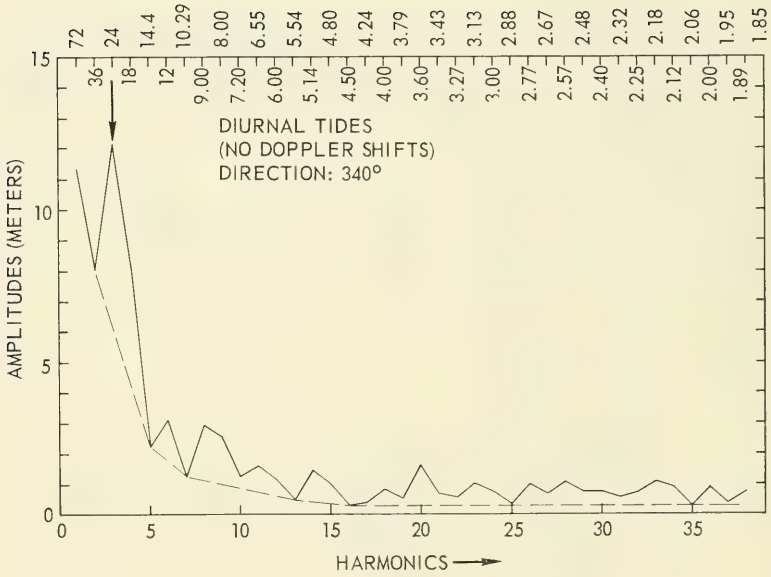

Figure 17. Mean amplitudes $\bar{A}_n$ for the upper 200 meters, San Diego- Honolulu. Set 7-9, 10 Aug 61, 2000 - 13 Aug 61, 2000.

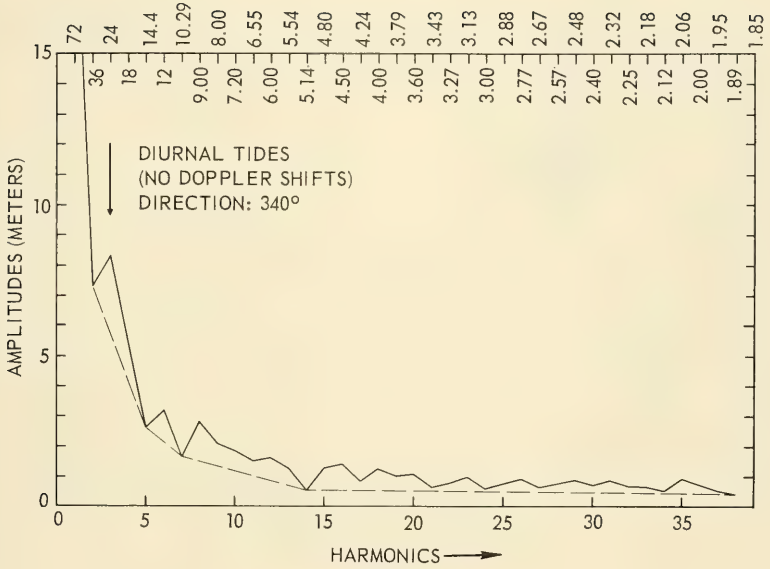

Figure 18. Mean amplitudes $\overline{A}_n$ for the upper 200 meters, San Diego-Honolulu. Set 8-10, 11 Aug 61, 2000 - 14 Aug 61, 2000.

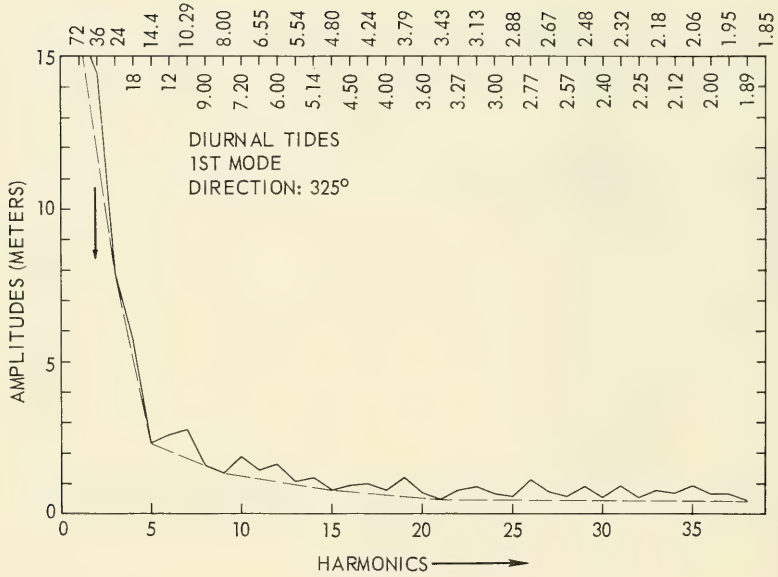

Figure 19. Mean amplitudes $\bar{A}_n$ for the upper 200 meters, San Diego-Honolulu. Set 9-11, 12 Aug 61, 2000 - 15 Aug 61, 2000.

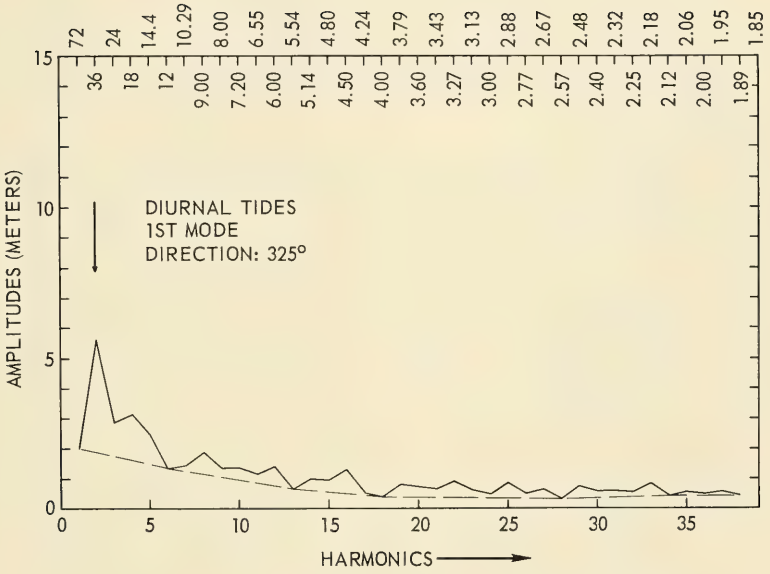

Figure 20. Mean amplitudes $\overline{A}_n$ for the upper 200 meters, San Diego- Honolulu. Set 10-12, 12 Aug 61, 2000- 16 Aug 61, 2000.

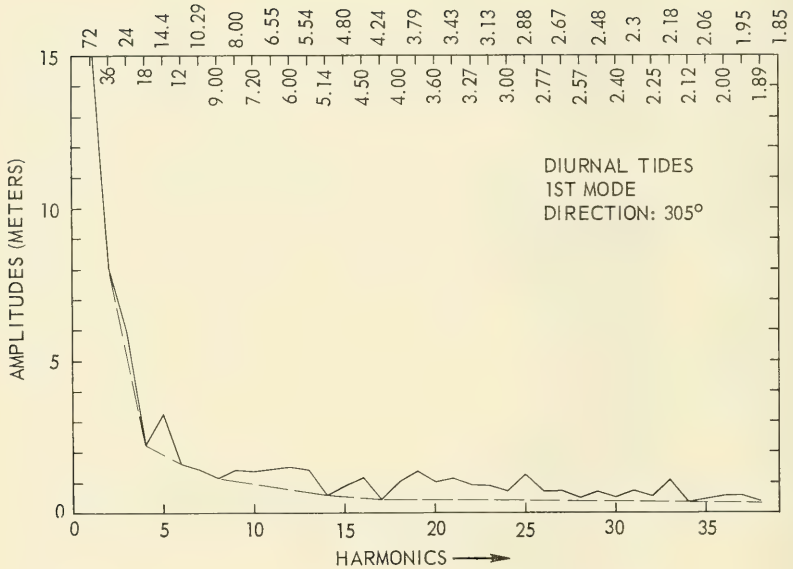

Figure 21. Mean amplitudes $\bar{A}_n$ for the upper 200 meters, San Diego - Honolulu. Set 11-13, 14 Aug 61, 2000 - 17 Aug 61, 2000.

$U = 6$ knots $= 3.1$ m/sec, $\cos \alpha = 0.2740$ is found. Therefore, the angle between the ship's direction (255°) and the direction of the internal diurnal tidal wave is 74°. The wave travels in either a northerly or a southeasterly direction. The northerly direction has been accepted in consideration of the surface tide.

The doppler shift up to the 5^{th} mode has been computed with the same angle, 74° (indicated by arrows in fig. 12). The determination of the direction of the semidiurnal internal waves has been carried out in the same way, assuming that the 12.4-hour period is shifted to the second group of peaks. The results are shown in figures 12-21.

The figures show that a systematic shift occurs: the diurnal internal tidal waves appear at periods between about 18 and 6 hours in sets 1-3, 2-4, 3-5, and 4-6, which represent positions north of 28° latitude. Therefore, they always travel in the same direction, namely, to the north. In set 6-8 a shift to 14.4 hours occurs but the waves in the following sets turn to the northwest, as indicated by the peak that occurs at 24 hours in sets 7-9 and 8-10, and at 36 hours in sets 9-11 and 10-12. In set 11-13 the peak seems to be shifted even further to the long-period range, which indicates that the wave has turned more into the ship's direction.

In regard to the semidiurnal internal tidal waves, one finds an angle of 67° between the ship's direction and the direction of wave travel. Again there is an uncertainty of $\pm \pi$ and the direction that agrees best with the direction of surface tides is accepted. This leads to 45° for the direction of internal wave progress.

The amplitudes in the semidiurnal range decrease with increasing set number; they cannot be recognized in the sets following set 4-6.

Figure 11 shows the ship's route, the analyzed direction of the diurnal (25 hour) and semidiurnal (12.4 hour) internal tidal waves and the cotidal lines of the semidiurnal surface tides (as given by G. Dietrich; see ref 13). The results in regard to semidiurnal internal tides agree with the theoretical concept given previously: *(1) in general they have the direction of the surface tides as long as these can be considered to be forced by the tide-generating force, and (2) their amplitude decreases toward Hawaii and their direction cannot be determined for the western part of the cruise, because two tidal domains seem to be present. There should be one internal tidal wave coming from the northwest and another one from the southeast; the latter belongs to the amphidromic system centered near 5°S, 155°W. Therefore, both waves may cancel or at least merge in such a way as to greatly reduce the amplitudes. The diurnal surface tides travel toward the west near Hawaii and in a northwesterly direction elsewhere on the ship's track, as shown in Dietrich's phase diagram for the surface tide.[13] This agrees with the expected directions south of 28°N. North of this latitude only internal Kelvin waves are possible, and since the coastline is north-south, it is expected that these waves would also travel in a south-to-north direction. This is very pronounced in all spectra north of 28°N.

---

*See pages 21-28.

CONCLUSIONS

The study has shown that the resolution of the Fourier amplitude spectra is not high enough to permit accepting them, and the conclusions they suggest, with complete confidence. The chain records do not permit interpretation of vertical changes in the amplitudes by the eigenfunctions. The actual density distribution is available to compute phase velocities of the internal waves in the area under consideration. However, the continous shift in the spectrum supports the theoretical results described in the section on forced internal waves (pp. 16-20). Therefore, the numerical results give a tentative picture which can be checked by additional measurement.

RECOMMENDATIONS

1. Verify the theory of internal waves of tidal period with additional measurements with the thermistor chain.
2. For a complete analysis of the various modes of internal waves, extend measurement of the thermal structure to the sea floor.
3. Supplement the study of internal waves by the use of current meters and salinometers mounted on the chain or at anchored stations; use the date produced to increase the usefulness of thermistor-chain data in the study of the ocean structure (sound-velocity structure) controlled by nonperiodic motion such as advection.

BIBLIOGRAPHY

1. Defant, A., "Reality and Illusion in Oceanographic Surveys," Journal of Marine Research, v. 9, p. 120-138, 1950
2. Reid, J.L., Jr., "Observations on Internal Tides in October 1950," American Geophysical Union. Transactions, v. 37, p. 278-286, June 1956
3. Rudnick, P. and Cochrane, J.D., "Diurnal Fluctuations in Bathythermograms," Journal of Marine Research, v. 10, p. 257-262, 1951
4. Emery, K.O., The Sea Off Southern California; A Modern Habitat of Petroleum, p. 126-130, Wiley, 1960
5. Arthur, R.S., "Oscillations in Sea Temperature at Scripps and Oceanside Piers," Deep-Sea Research, v. 2, p. 107-121, 1954
6. Lee, O.S., "Observations on Internal Waves in Shallow Water," Limnology and Oceanography, v. 6, p. 312-321, July 1961

7. Summers, H.J. and Emery, K.O., "Internal Waves of Tidal Period Off Southern California," Journal of Geophysical Research, v. 68, p. 827-839, 1 February 1963

8. Navy Electronics Laboratory Report 1114, The USNEL Thermistor Chain, by E.C. LaFond, 20 June 1962

9. Defant, A., "The Origin of Internal Tide Waves in the Open Sea," Journal of Marine Research, v. 9, p. 111-119, 1950

10. Haurwitz, B., "Internal Waves of Tidal Character," American Geophysical Union. Transactions, v. 31, p. 47-52, February 1950

11. Navy Electronics Laboratory Report 1130, Measurements of Thermal Structure Off Southern California With the NEL Thermistor Chain, by E.C. LaFond and A.T. Moore, 28 August 1962

12. Oceanic Observations of the Pacific: 1955, The NORPAC ATLAS: (prepared by the NORPAC Committee) Berkeley, University of California Press, Tokyo, University of Tokyo Press, 1960, fig. 83

13. Dietrich, G., "Die Schwingungssysteme der Halb-und Eintägigen Tiden in den Ozeanen," Berlin. Universität. Institut für Meereskunde. Veröffentlichungen. Series A. Geographisch-Naturwissenschaftliche Reihe, v. 41, 1944

Groen, P., "Contribution to the Theory of Internal Waves," Koninklijk Nederlands Meteorologisch Instituut de Bilt. Mededelingen en Verhandelingen, Ser. B, v. 2, No. 11, 1948

Lockheed Aircraft Corporation Report LR 16795, Spectra of Internal Waves Over Basins and Banks Off Southern California, by A.J. Carsola and others, March 1963

UNCLASSIFIED
Security Classification

DOCUMENT CONTROL DATA - R&D
(Security classification of title, body of abstract and indexing annotation must be entered when the overall report is classified)

1. ORIGINATING ACTIVITY *(Corporate author)*
Navy Electronics Laboratory
San Diego, California 92152

2a. REPORT SECURITY CLASSIFICATION
UNCLASSIFIED

2b. GROUP

3. REPORT TITLE
INTERNAL TIDES OFF SOUTHERN CALIFORNIA

4. DESCRIPTIVE NOTES *(Type of report and inclusive dates)*
Research and Development Report, August 1963-February 1964

5. AUTHOR(S) *(Last name, first name, initial)*
Krauss, W.

6. REPORT DATE	7a. TOTAL NO. OF PAGES	7b. NO. OF REFS
6 July 1966	53	15

8a. CONTRACT OR GRANT NO.	9a. ORIGINATOR'S REPORT NUMBER(S)
b. PROJECT NO. SR 104 03 01, Task 0580 (NEL L40461)	1389
c.	9b. OTHER REPORT NO(S) *(Any other numbers that may be assigned this report)*
d.	

10. AVAILABILITY/LIMITATION NOTICES
Distribution of this document is unlimited.

11. SUPPLEMENTARY NOTES	12. SPONSORING MILITARY ACTIVITY
	Naval Ship Systems Command Department of the Navy

13. ABSTRACT

A method accounting for doppler-shift effects was used to interpret data recorded from San Diego to Hawaii by moving thermistors. Results lead to a reasonable picture of the internal tides in that area of the Pacific Ocean. Internal tidal waves are an important component in the spectra at tidal frequencies in the sea off southern California. It is likely that they travel in a northeasterly direction.

DD FORM 1 JAN 64 1473 0101-807-6800

UNCLASSIFIED
Security Classification

14. KEY WORDS	LINK A		LINK B		LINK C	
	ROLE	WT	ROLE	WT	ROLE	WT
Tides - Pacific Ocean						
Internal Waves						

INSTRUCTIONS

1. ORIGINATING ACTIVITY: Enter the name and address of the contractor, subcontractor, grantee, Department of Defense activity or other organization *(corporate author)* issuing the report.

2a. REPORT SECURITY CLASSIFICATION: Enter the overall security classification of the report. Indicate whether "Restricted Data" is included. Marking is to be in accordance with appropriate security regulations.

2b. GROUP: Automatic downgrading is specified in DoD Directive 5200.10 and Armed Forces Industrial Manual. Enter the group number. Also, when applicable, show that optional markings have been used for Group 3 and Group 4 as authorized.

3. REPORT TITLE: Enter the complete report title in all capital letters. Titles in all cases should be unclassified. If a meaningful title cannot be selected without classification, show title classification in all capitals in parenthesis immediately following the title.

4. DESCRIPTIVE NOTES: If appropriate, enter the type of report, e.g., interim, progress, summary, annual, or final. Give the inclusive dates when a specific reporting period is covered.

5. AUTHOR(S): Enter the name(s) of author(s) as shown on or in the report. Enter last name, first name, middle initial. If military, show rank and branch of service. The name of the principal author is an absolute minimum requirement.

6. REPORT DATE: Enter the date of the report as day, month, year, or month, year. If more than one date appears on the report, use date of publication.

7a. TOTAL NUMBER OF PAGES: The total page count should follow normal pagination procedures, i.e., enter the number of pages containing information.

7b. NUMBER OF REFERENCES: Enter the total number of references cited in the report.

8a. CONTRACT OR GRANT NUMBER: If appropriate, enter the applicable number of the contract or grant under which the report was written.

8b, 8c, & 8d. PROJECT NUMBER: Enter the appropriate military department identification, such as project number, subproject number, system numbers, task number, etc.

9a. ORIGINATOR'S REPORT NUMBER(S): Enter the official report number by which the document will be identified and controlled by the originating activity. This number must be unique to this report.

9b. OTHER REPORT NUMBER(S): If the report has been assigned any other report numbers *(either by the originator or by the sponsor)*, also enter this number(s).

10. AVAILABILITY/LIMITATION NOTICES: Enter any limitations on further dissemination of the report, other than those imposed by security classification, using standard statements such as:

(1) "Qualified requesters may obtain copies of this report from DDC."

(2) "Foreign announcement and dissemination of this report by DDC is not authorized."

(3) "U. S. Government agencies may obtain copies of this report directly from DDC. Other qualified DDC users shall request through

_____."

(4) "U. S. military agencies may obtain copies of this report directly from DDC. Other qualified users shall request through

_____."

(5) "All distribution of this report is controlled. Qualified DDC users shall request through

_____."

If the report has been furnished to the Office of Technical Services, Department of Commerce, for sale to the public, indicate this fact and enter the price, if known.

11. SUPPLEMENTARY NOTES: Use for additional explanatory notes.

12. SPONSORING MILITARY ACTIVITY: Enter the name of the departmental project office or laboratory sponsoring *(paying for)* the research and development. Include address.

13. ABSTRACT: Enter an abstract giving a brief and factual summary of the document indicative of the report, even though it may also appear elsewhere in the body of the technical report. If additional space is required, a continuation sheet shall be attached.

It is highly desirable that the abstract of classified reports be unclassified. Each paragraph of the abstract shall end with an indication of the military security classification of the information in the paragraph, represented as *(TS)*, *(S)*, *(C)*, or *(U)*.

There is no limitation on the length of the abstract. However, the suggested length is from 150 to 225 words.

14. KEY WORDS: Key words are technically meaningful terms or short phrases that characterize a report and may be used as index entries for cataloging the report. Key words must be selected so that no security classification is required. Identifiers, such as equipment model designation, trade name, military project code name, geographic location, may be used as key words but will be followed by an indication of technical context. The assignment of links, roles, and weights is optional.

Navy Electronics Lab., San Diego, Calif.
Report 1389

INTERNAL TIDES OFF SOUTHERN CALIFORNIA, by W. Krauss, 53 p., 6 Jul 66.

UNCLASSIFIED

A method accounting for doppler-shift effects was used to interpret data recorded from San Diego to Hawaii by moving thermistors. Results lead to a reasonable picture of the internal tides in that area of the Pacific Ocean. Internal tidal waves are an important component in the spectra at tidal frequencies in the sea off southern California. It is likely that they travel in a northeasterly direction.

1. Tides - Pacific Ocean
2. Internal Waves

I. Krauss, W.

SR 104 03 01, Task 0580
(NEL L40461)

This card is UNCLASSIFIED

Navy Electronics Lab., San Diego, Calif.
Report 1389

INTERNAL TIDES OFF SOUTHERN CALIFORNIA, by W. Krauss, 53 p., 6 Jul 66.

UNCLASSIFIED

A method accounting for doppler-shift effects was used to interpret data recorded from San Diego to Hawaii by moving thermistors. Results lead to a reasonable picture of the internal tides in that area of the Pacific Ocean. Internal tidal waves are an important component in the spectra at tidal frequencies in the sea off southern California. It is likely that they travel in a northeasterly direction.

1. Tides - Pacific Ocean
2. Internal Waves

I. Krauss, W.

SR 104 03 01, Task 0580
(NEL L40461)

This card is UNCLASSIFIED

Navy Electronics Lab., San Diego, Calif.
Report 1389

INTERNAL TIDES OFF SOUTHERN CALIFORNIA, by W. Krauss, 53 p., 6 Jul 66.

UNCLASSIFIED

A method accounting for doppler-shift effects was used to interpret data recorded from San Diego to Hawaii by moving thermistors. Results lead to a reasonable picture of the internal tides in that area of the Pacific Ocean. Internal tidal waves are an important component in the spectra at tidal frequencies in the sea off southern California. It is likely that they travel in a northeasterly direction.

1. Tides - Pacific Ocean
2. Internal Waves

I. Krauss, W.

SR 104 03 01, Task 0580
(NEL L40461)

This card is UNCLASSIFIED

Navy Electronics Lab., San Diego, Calif.
Report 1389

INTERNAL TIDES OFF SOUTHERN CALIFORNIA, by W. Krauss, 53 p., 6 Jul 66.

UNCLASSIFIED

A method accounting for doppler-shift effects was used to interpret data recorded from San Diego to Hawaii by moving thermistors. Results lead to a reasonable picture of the internal tides in that area of the Pacific Ocean. Internal tidal waves are an important component in the spectra at tidal frequencies in the sea off southern California. It is likely that they travel in a northeasterly direction.

1. Tides - Pacific Ocean
2. Internal Waves

I. Krauss, W.

SR 104 03 01, Task 0580
(NEL L40461)

This card is UNCLASSIFIED

INITIAL DISTRIBUTION LIST

CHIEF OF NAVAL MATERIAL
MAT 033
COMMANDER, NAVAL SHIP SYSTEMS COMMAND
SHIPS 1610
SHIPS 1620
SHIPS 1631
SHIPS 2021 (2)
SHIPS 204113
COMMANDER, NAVAL FACILITIES ENGINEERING COMMAND
CODE 42310
COMMANDER, NAVAL AIR SYSTEMS COMMAND
AIR 5330
AIR 5330 (RUDC-2)
AIR 5330 (RUDC-3)
COMMANDER, NAVAL ORDNANCE SYSTEMS COMMAND
ORD 9132
ORD 9132 (DLI-304)
ORD 03C
ORD 0322
FASS
COMMANDER, NAVAL SHIP ENGINEERING CENTER
CODE 6420
CODE 6440
CODE 6452E
CODE 6454
CHIEF OF NAVAL PERSONNEL
PERS 11B
CHIEF OF NAVAL OPERATIONS
OP-312 F
OP-07T
OP-701
OP-71
OP-03EG
OP-098S
OP-311
OP-322C
OP-702C
OP 716
OP-922Y4C1
CHIEF OF NAVAL RESEARCH
CODE 416
CODE 418
CODE 427
CODE 466
CODE 468
CODE 493
COMMANDER IN CHIEF US PACIFIC FLEET
COMMANDER IN CHIEF US ATLANTIC FLEET
COMMANDER OPERATIONAL TEST AND EVALUATION FORCE
DEPUTY COMMANDER OPERATIONAL TEST + EVALUATION FORCE, PACIFIC
COMMANDER SUBMARINE FORCE
US PACIFIC FLEET
US ATLANTIC FLEET
DEPUTY COMMANDER SUBMARINE FORCE, US ATLANTIC FLEET
COMMANDER ANTISUBMARINE WARFARE FOR US PACIFIC FLEET
COMMANDER FIRST FLEET
COMMANDER SECOND FLEET
COMMANDER TRAINING COMMAND US ATLANTIC FLEET
OCEANOGRAPHIC SYSTEM PACIFIC
COMMANDER SUBMARINE DEVELOPMENT GROUP TWO
COMMANDER KEY WEST TEST + EVALUATION DETACHMENT
DESTROYER DEVELOPMENT GROUP PACIFIC
FLEET AIR WINGS, ATLANTIC FLEET
SCIENTIFIC ADVISORY TEAM
US NAVAL AIR DEVELOPMENT CENTER
NADC LIBRARY
US NAVAL MISSILE CENTER
TECH. LIBRARY
PACIFIC MISSILE RANGE /CODE 3250/
US NAVAL ORDNANCE LABORATORY
LIBRARY
SYSTEMS ANALYSIS GROUP OF THE ASW R-D PLANNING COUNCIL, CODE RA
US NAVAL ORDNANCE TEST STATION
PASADENA ANNEX LIBRARY
CHINA LAKE

ABERDEEN PROVING GROUND, MD. 21005
REDSTONE SCIENTIFIC INFORMATION CENTER
US ARMY ELECTRONICS R-D LABORATORY
AMSEL-RD-MAT
COASTAL ENGINEERING RESEARCH CENTER
CORPS OF ENGINEERS, US ARMY
HEADQUARTERS, US AIR FORCE
AFRSTA
AIR UNIVERSITY LIBRARY
AIR FORCE EASTERN TEST RANGE /AFMTC TECH LIBRARY - MU-135/
AIR PROVING GROUND CENTER, PGBPS-12
HQ AIR WEATHER SERVICE
WRIGHT-PATTERSON AF BASE
SYSTEMS ENGINEERING GROUP (RTD)
UNIVERSITY OF MICHIGAN
OFFICE OF RESEARCH ADMINISTRATION
UNIVERSITY OF MIAMI
THE MARINE LAB. LIBRARY
MICHIGAN STATE UNIVERSITY
COLUMBIA UNIVERSITY
HUDSON LABORATORIES
LAMONT GEOLOGICAL OBSERVATORY
DARTMOUTH COLLEGE
RADIOPHYSICS LABORATORY
CALIFORNIA INSTITUTE OF TECHNOLOGY
JET PROPULSION LABORATORY
HARVARD COLLEGE OBSERVATORY
OREGON STATE UNIVERSITY
DEPARTMENT OF OCEANOGRAPHY
UNIVERSITY OF WASHINGTON
DEPARTMENT OF OCEANOGRAPHY
FISHERIES-OCEANOGRAPHY LIBRARY
NEW YORK UNIVERSITY
DEPT OF METEOROLOGY + OCEANOGRAPHY
UNIVERSITY OF MICHIGAN
DIRECTOR, COOLEY ELECTRONICS LAB
DR. JOHN C. AYERS
UNIVERSITY OF WASHINGTON
DIRECTOR, APPLIED PHYSICS LABORATORY
OHIO STATE UNIVERSITY
PROFESSOR L. E. BOLLINGER
UNIVERSITY OF ALASKA
GEOPHYSICAL INSTITUTE
UNIVERSITY OF RHODE ISLAND
NARRAGANSETT MARINE LABORATORY
YALE UNIVERSITY
BINGHAM OCEANOGRAPHIC LABORATORY
FLORIDA STATE UNIVERSITY
OCEANOGRAPHIC INSTITUTE
UNIVERSITY OF HAWAII
HAWAII INSTITUTE OF GEOPHYSICS
ELECTRICAL ENGINEERING DEPT
HARVARD UNIVERSITY
GORDON MCKAY LIBRARY
A+M COLLEGE OF TEXAS
DEPARTMENT OF OCEANOGRAPHY
THE UNIVERSITY OF TEXAS
DEFENSE RESEARCH LABORATORY
ELECTRICAL ENGINEERING RESEARCH LAB
HARVARD UNIVERSITY
UNIVERSITY OF CALIFORNIA-SAN DIEGO
SCRIPPS INSTITUTION OF OCEANOGRAPHY
MARINE PHYSICAL LAB
PENNSYLVANIA STATE UNIVERSITY
ORDNANCE RESEARCH LABORATORY
NAVAL WARFARE RESEARCH CENTER
STANFORD RESEARCH INSTITUTE
MASSACHUSETTS INST OF TECHNOLOGY
ENGINEERING LIBRARY
MIT-LINCOLN LABORATORY
RADIO PHYSICS DIVISION
THE JOHNS HOPKINS UNIVERSITY
APPLIED PHYSICS LABORATORY
INSTITUTE FOR DEFENSE ANALYSES
FLORIDA ATLANTIC UNIVERSITY
US NAVAL WEAPONS LABORATORY
KXL
LIBRARY
PEARL HARBOR NAVAL SHIPYARD
PORTSMOUTH NAVAL SHIPYARD
PUGET SOUND NAVAL SHIPYARD
SAN FRANCISCO NAVAL SHIPYARD

USN RADIOLOGICAL DEFENSE LABORATORY
DAVID TAYLOR MODEL BASIN /LIBRARY/
US NAVY MINE DEFENSE LABORATORY
US NAVAL TRAINING DEVICE CENTER
CODE 365H, ASW DIVISION
USN UNDERWATER SOUND LABORATORY
LIBRARY
CODE 905
ATLANTIC FLEET ASW TACTICAL SCHOOL
USN MARINE ENGINEERING LABORATORY
US NAVAL CIVIL ENGINEERING LAB.
L54
US NAVAL RESEARCH LABORATORY
CODE 2027
CODE 5440
US NAVAL ORDNANCE LABORATORY
CORONA
USN UNDERWATER SOUND REFERENCE LAB.
US FLEET ASW SCHOOL
US FLEET SONAR SCHOOL
USN UNDERWATER WEAPONS RSCH & ENG. STATION
OFFICE OF NAVAL RESEARCH
PASADENA
US NAVAL SHIP MISSILE SYSTEMS ENGINEERING STATION
CHIEF OF NAVAL AIR TRAINING
USN WEATHER RESEARCH FACILITY
US NAVAL OCEANOGRAPHIC OFFICE
SUPERVISOR OF SHIPBUILDING US NAVY GROTON
US NAVAL POSTGRADUATE SCHOOL
LIBRARY(CODE 0384)
DEPT. OF ENVIRONMENTAL SCIENCES
OFFICE OF NAVAL RESEARCH BR OFFICE
LONDON
BOSTON
CHICAGO
SAN FRANCISCO
FLEET NUMERICAL WEATHER FACILITY
US NAVAL APPLIED SCIENCE LABORATORY
CODE 9200, ELECTRONICS DIVISION
CODE 9832
US NAVAL ACADEMY
ASSISTANT SECRETARY OF THE NAVY R+D
US NAVAL SECURITY GROUP HDQTRS(G43)
ONR SCIENTIFIC LIAISON OFFICER
WOODS HOLE OCEANOGRAPHIC INSTITUTION
INSTITUTE OF NAVAL STUDIES
LIBRARY
AIR DEVELOPMENT SQUADRON ONE /VX-1/
SUBMARINE FLOTILLA ONE
DEFENSE DOCUMENTATION CENTER (20)
DOD RESEARCH AND ENGINEERING
WEAPONS SYSTEMS EVALUATION GROUP
DEFENSE ATOMIC SUPPORT AGENCY
NATIONAL OCEANOGRAPHIC DATA CENTER
US COAST GUARD OCEANOGRAPHIC UNIT
COMMITTEE ON UNDERSEA WARFARE
US COAST GUARD HDQTRS(OSR-2)
ARCTIC RESEARCH LABORATORY
WOODS HOLE OCEANOGRAPHIC INSTITUTION
US COAST AND GEODETIC SURVEY
WASHINGTON SCIENCE CENTER - 23
FEDERAL COMMUNICATIONS COMMISSION
US WEATHER BUREAU
DIRECTOR, METEOROLOGICAL RESEARCH LIBRARY
NATIONAL SEVERE STORMS LABORATORY
NORMAN, OKLAHOMA 73069
NATIONAL BUREAU OF STANDARDS
BOULDER LABORATORIES
US GEOLOGICAL SURVEY LIBRARY
DENVER SECTION
US BUREAU OF COMMERCIAL FISHERIES
LA JOLLA
WASHINGTON, D. C. 20240
WOODS HOLE, MASSACHUSETTS 02543
HONOLULU, HAWAII 96812
STANFORD, CALIFORNIA 94305
TUNA RESOURCES LAB LA JOLLA